Annu. Rev. Astron. Astrophys. 1994. 32: 531–590

BARYONIC DARK MATTER

Bernard Carr

Schools of Mathematical Sciences, Queen Mary and Westfield College, Mile End Road, London E1 4NS, England

KEY WORDS: black holes, Population III stars, background radiation, gravitational lensing, brown dwarfs

1. INTRODUCTION

The evidence for dark matter, on all scales from star clusters ($10^6 M_\odot$) to the Universe itself ($10^{22} M_\odot$), has built up steadily over the past 50 years (Faber & Gallagher 1979, Trimble 1987, Turner 1991, Ashman 1992). Although the strength of the evidence on different scales varies considerably, there is now little doubt that only a small fraction of the mass of the Universe is in visible form. However, we remain uncertain as to the identity of the dark material. Proposed candidates span the entire mass range from 10^{-5}eV to $10^{12} M_\odot$, with a dichotomy between those—primary particle physicists—who would like the dark matter to be some sort of elementary particle and those—primarily astrophysicists—who would prefer it to be some sort of astrophysical object. In the first case, the dark matter would have to be nonbaryonic, with the particles being relics from the hot Big Bang; in the second case, it would have to be baryonic, with the dark objects being made out of gas which has been processed into the remnants of what are sometimes termed "Population III" stars.

During the 1970s the dark matter was usually assumed, at least implicitly, to be baryonic (e.g. Ostriker et al 1974, White & Rees 1978), but in the 1980s attention veered towards the nonbaryonic candidates. This was partly because of developments in particle physics, but also because it was realized that there are good cosmological reasons for believing that not everything can be baryonic (Hegyi & Olive 1983, 1986). For a while "hot" dark matter was popular, but soon "cold" dark matter took center stage and many people still regard this as the "standard" model. In the past few years, however, attention has returned to the baryonic candidates—partly because of perceived problems in the cold model and also because there may now be direct evidence for baryonic dark

0066–4146/94/0915–0531$05.00

matter. Entire conferences are now devoted to the topic (e.g. Lynden-Bell & Gilmore 1990), and there seems to be a growing realization that there are so many dark matter problems that one probably needs *both* baryonic and nonbaryonic solutions.

This review focuses almost exclusively on baryonic dark matter. Section 2 presents the observational evidence for dark matter in various contexts; the discussion here is rather brief because it is only necessary to highlight those issues that relate to baryonic dark matter in particular. Section 3 reviews the general arguments for baryonic and nonbaryonic dark matter, concluding—as indicated above—that one probably needs both. Section 4 discusses *why* one expects baryonic dark matter to form; this involves a brief review of the "Population III" scenario. Section 5 summarizes the constraints on the Population III scenario which come from background light and nucleosynthetic considerations. These limits are essentially as described by Carr et al (1984) but Sections 6 and 7 focus on topics—dynamical effects and lensing effects—that have seen important recent developments. The most plausible candidates seem to be the black hole remnants of high mass stars or low mass objects, so we focus on these candidates in more detail in Sections 8 and 9, respectively. We conclude in Section 10 with a reappraisal of these and other candidates and we assess the prospects of finding or excluding them.

2. EVIDENCE FOR DARK MATTER

The observational evidence for dark matter arises in many different contexts and baryonic dark matter is not necessarily inplicated in all of these. We therefore begin by identifying the observational issues most relevant to the baryonic versus nonbaryonic dilemma.

2.1 *Local Dark Matter*

Measurements of the stellar velocity and density distribution perpendicular to the Galactic disk provide an estimate of the total disk density. This turns out to be about 0.1 $M_\odot \mathrm{pc}^{-3}$ and it has long been suspected (Oort 1932) that this exceeds the density in visible stars. *The possibility of disk dark matter is very important in the present context because—of all the dark matter problems—this is the one most likely to have a baryonic solution.* Unfortunately, the evidence is very controversial. Bahcall (1984a,b,c) used counts of F dwarfs and K giants to conclude that the density of unseen material must be at least 50% that of the visible material. He also concluded that the disk dark matter must have an exponential scale height of less than 700 pc, so that it must itself be confined to a disk. However, Bahcall assumed a particular model and Bienayme et al (1987), using a different model, found a best-fit dark matter density of only $0.01 M_\odot \mathrm{pc}^{-3}$, and even this could be removed if the halo was slightly flattened.

Knapp (1988) came to the same conclusion by studying the velocity dispersion and scale height of molecular hydrogen. Further doubt was cast in a series of papers by Kuijken & Gilmore (1989), who used the full distribution function for the velocities and distances of K dwarfs rather than assuming a particular model. Although Gould (1990) used a maximum likelihood analysis to conclude that Kuijken & Gilmore's data were not inconsistent with the Bahcall et al claim, Kuijken & Gilmore (1991) disagreed with this. More recently, Bahcall et al (1992a) have concluded from another analysis of K giants that the no-disk-dark-matter hypothesis is only consistent with the data at the 14% level and their best-fit model has a dark density of 0.15 $M_{\odot}\text{pc}^{-3}$, which corresponds to 53% more dark matter than visible matter. For present purposes the existence of disk dark matter will be regarded as an open question.

2.2 *Spiral Galaxies*

The best evidence for dark matter in galaxies comes from the rotation curves of spirals, since the dependence of the rotation speed V upon galactocentric distance R is a measure of the density profile $\rho(R)$. An important feature of our own and many other spiral galaxies is that the rotation speed, after an initital rise, remains approximately constant with increasing R (Rubin et al 1980). This implies that the mass within radius R increases like R, which is faster than the increase of visible mass. [Valentjin (1990) has claimed that spiral galaxies have sufficient dust to be opaque, thereby increasing the stellar mass content (cf Disney et al 1989), but Burstein et al (1991) disagree with this and the possibility will be neglected here.] Although the dark matter does not dominate within the optical galaxy (at least for bright galaxies), neutral hydrogen observations suggest that V continues to remain constant well beyond the visible stars (Sancisi & van Albada 1987). *In considering the baryonic contribution to galactic halos, the crucial issue is how far the halos extend.* For our galaxy the minimum halo radius consistent with rotation curve measurements, the local escape speed, and the kinematics of globular clusters and satellite galaxies is 35 kpc; the dynamics of the Magellanic Stream and the Local Group of galaxies may require a halo radius of 70 kpc (Fich & Tremaine 1991). We will see later that these values are marginally consistent with a baryonic halo. However, Zaritsky et al (1993) argue from observations of satellite systems that spiral galaxies typically have 200 kpc halos and this would be inconsistent with their being composed of baryons.

One indication that halos are dominated by nonbaryonic material may come from the fact that V has the same value in the optical region (where the bulge and disk dominate) as it does well beyond (where the dark matter dominates). This "conspiracy" may require that the ratio of baryonic to nonbaryonic dark mass be comparable to the dimensionless rotation parameter expected for protogalaxies as a result of tidal spinup (Fall & Efstathiou 1981, Blumenthal et al 1986);

both are of order 0.1. A recent calculation of this effect, allowing for the response of the dark halo to the dissipative infall of the luminous material, implies a baryonic to nonbaryonic ratio of 0.05 (Flores et al 1993). However, this would not apply if the baryons went dark before galaxy formation. Also, the conspiracy is only required for bright galaxies because only for these is the disk dynamically dominant in the central regions.

Another relevant issue concerns the *roundness* of galactic halos. If galactic halos are baryonic, one would expect their formation to involve dissipation, in which case they should be flatter than in the nonbaryonic case: *N*-body experiments show that dissipationless collapse does give some flattening but the resultant triaxial halos are rarely flatter than E6 (Frenk et al 1988, Dubinski & Carlberg 1991). Thus, evidence for halos flatter than this would be evidence for baryonic dark matter. Polar ring galaxies probably provide the best probe of halo shape, and these do seem to indicate triaxiality (Whitmore et al 1987), sometimes (e.g. for NGC 4650A) as high as E6 (Sackett & Sparke 1990). The existence of warped disks may also require triaxial surrounding halos (Teuben 1991), and such disks seem to be ubiquitous (Bosma 1991). Triaxiality in our own halo could also explain the asymmetries of the HI distribution (Blitz & Spergel 1991). Nevertheless, it is not clear whether there is enough triaxiality in these cases to imply baryonic halos.

2.3 *Elliptical Galaxies*

The mass distribution in ellipticals can be probed by measuring the velocity dispersion of the stars and globular clusters. Unfortunately, the velocities do not determine the density profile uniquely and this method gives no evidence for dark matter within the *central* regions of ellipticals (de Zeeuw 1992), although the dynamics of globular clusters does provide evidence for dark matter around M87 (Huchra & Brodie 1987, Mould et al 1990). The best information therefore comes from X-ray observations of hot gas. These do, in fact, provide evidence for dark matter and, in many cases, one finds the same $M \sim R$ law that characterizes spirals (Forman et al 1985, Sarazin 1986). Although these analyses assume that the gas is isothermal, usually one only has poor information on the temperature profile. However, Fabian et al (1986) obtain even larger minimum masses on the assumption that the halo is confined by a hydrostatic outer atmosphere. Giant ellipticals are sometimes the focus of cooling flows and this suggests that at least some of the dark matter in ellipticals may be baryonic (Fabian 1994).

2.4 *Dwarf Galaxies*

Some of the dwarf irregulars are extremely gas-rich, which means that their HI rotation curves can be traced to many optical scale lengths. Many of them seem to have much higher dark mass fractions than bright spirals, with their dark halos dominating even within the optical regions. Particularly striking examples are DDO 154 (Carignan & Freeman 1988), for which the dark-to-luminous mass ratio exceeds 10 at the last measured point of the rotation curve, GR 8 (Carignan et al 1990), and DDO 170 (Lake et al 1990). Dwarf spheroidals also seem to have dark halos (Lin & Faber 1983, Aaronson 1983, Aaronson & Olszewski 1987). This claim is based on measurements of velocity dispersions and tidal radii for the six dwarf spheroidals within the Local Group. Originally the dispersions had to be inferred from the individual velocities of only a dozen or so objects per galaxy, but higher resolution velocity measurements now provide much better data (Mateo et al 1991) and seem to confirm the results of the earlier work. *The presence of dark matter in dwarf galaxies is crucial in the present context because it requires that halos consist either of baryonic or cold nonbaryonic dark matter.* Lake (1990) has argued that the observations are more consistent with the first possibility: If the formation of the halos were dissipationless, their central densities imply that the galaxies need to form at a redshift exceeding 30, whereas they should form at a redshift of 10 in the Cold Dark Matter (CDM) scenario.

2.5 *Groups and Clusters of Galaxies*

Galaxies are clumped on various scales (as members of binaries, small groups, and rich clusters) and velocity dispersion measurements indicate that the dynamical mass exceeds the visible mass on all these scales. Binaries can only be studied statistically (because one does not know the orbital inclination in any individual case), so the data are less clear-cut here; however, there is compelling evidence for dark mass in clusters of galaxies. This is confirmed by X-ray data on the gas temperature (which provide an independent measure of the gravitational potential). In rich clusters, the dark mass dominates by at least a factor of 10 and the recent discovery of hot gas in two *small* groups of galaxies (HG92 and HCG62) by *ROSAT* shows that there are comparable amounts of dark matter there (Mulchaey et al 1993, Ponman & Bertram 1993).

In assessing whether the dark mass in groups and clusters can be baryonic, it is important to determine whether it is the same as the halo dark matter. Although the cluster dark mass cannot all be associated with individual galaxies *now*—for then dynamical friction would result in the most massive galaxies being dragged into the cluster center (White 1976)—it may still have derived from the galaxies originally. Indeed, in the hierarchial clustering picture one would expect the galaxies inside a cluster to be stripped of their individual halos to form a collective halo (White & Rees 1978). However, this would only suffice to explain all the cluster dark matter if the original galactic halos were larger than about 200 kpc and, in this case, we will see that they could not be purely baryonic unless one invokes inhomogeneous Big Bang nucleosynthesis.

2.6 *Background Dark Matter*

None of the forms of matter discussed above can have the critical density required for the Universe to recollapse: $\rho_{\rm crit} = 3H_o^2/8\pi G = 2 \times 10^{-29}h^{-2}$ g cm^{-3}, where $h = H_o/(100$ km s^{-1} Mpc$^{-1})$. As discussed later, disk dark matter could only have $\Omega_d \sim 0.001$, while the halo and cluster dark matter could only have $\Omega_{\rm h} \sim 0.01$–0.1 and $\Omega_{\rm c} \sim 0.1$–0.2, respectively. However, according to the currently popular inflation theory (Guth 1981), in which the Universe undergoes an exponential expansion phase at some early time, the total density should have almost exactly the critical value ($\Omega = 1$). [See, however, Ellis (1988) and Ellis et al (1991) for a different point of view.] This would have two possible implications: 1. There is another dark component, or 2. galaxy formation is biased (Kaiser 1984, Dekel & Rees 1987) in the sense that galaxies form preferentially in just a small fraction of the volume of the Universe. Although the second possibility avoids a proliferation of dark matter species, some people now invoke a mixture of hot and cold dark matter anyway (e.g. Taylor & Rowan-Robinson 1992).

In either case, one would expect the mass-to-light ratio to increase as one goes to larger scales, and there is some indication of this from dynamical studies. One can probe the density on scales above 10 Mpc, for example, by analyzing large-scale streaming motions (Dressler et al 1987, Bertschinger & Dekel 1989) or by determining the dipole moment of the *IRAS* sources (Rowan-Robinson et al 1990). In all these analyses, the inferred density depends on the bias parameter b (dynamical effects depending on the product $\Omega^{0.6}b^{-1}$). More sophisticated analyses are needed to determine Ω and b separately (Peacock & Dodds 1994, Nusser & Dekel 1993). The *IRAS* dipole suggests a critical density if the *IRAS* sources are unbiased ($b = 1$); however, this conclusion would be erroneous if there was a significant contribution to the dipole from distances beyond 100 Mpc (Scaramella et al 1991). For a recent review of the evidence for and against $\Omega = 1$, see Coles & Ellis (1994).

3. BARYONIC VS NONBARYONIC DARK MATTER

Candidates for the dark matter may be grouped into nonbaryonic and baryonic types. These will be referred to these as "Inos" and "Population III", respectively, and the candidates are listed explicitly in Table 1 in order of increasing mass. Some of the ino candidates are elementary particles and—depending on their mass—these are usefully classified as "hot" or "cold" since this affects their clustering properties. The term *Weakly Interacting Massive Particle* or *WIMP* is often used to describe these particles, though some people restrict this term to particles that are massive enough to be cold. The other inos are more exotic relics from the Big Bang and, for present purposes, primordial black holes are included in this category. [For a comprehensive review of the ino

Table 1 Baryonic and nonbaryonic matter candidates

INOS		POPULATION III	
Axions	(10^{-5} eV)	Snowballs	?
Neutrinos	(10 eV)	Brown dwarfs	($<0.08\ M_\odot$)
Photinos	(1 GeV)	M-dwarfs	($0.1\ M_\odot$)
Monopoles	(10^{16} GeV)	White dwarfs	($1\ M_\odot$)
Planck relicts	(10^{19} GeV)	Neutron stars	($2\ M_\odot$)
Primordial holes	($>10^{15}$ g)	Stellar holes	($\sim 10\ M_\odot$)
Quark nuggets	($< 10^{20}$ g)	VMO holes	(10^2–$10^5\ M_\odot$)
Shadow matter	?	SMO holes	($>10^5\ M_\odot$)

candidates, see Turner (1991).] Table 1 illustrates that there are many forms of nonluminous matter, so it is naive to assume that all the dark matter problems will have a single explanation. Even though some of the candidates in Table 1 can probably be rejected, many viable ones remain.

3.1 *Cosmological Nucleosynthesis*

The main argument for nonbaryonic dark matter is associated with Big Bang nucleosynthesis. This is because the success of the standard picture in explaining the primordial light element abundances [$X(^4\mathrm{He}) \approx 0.24$, $X(^2\mathrm{D}) \sim X(^3\mathrm{He}) \sim 10^{-5}$, $X(^7\mathrm{Li}) \sim 10^{-10}$] only applies if the baryon density parameter Ω_b is strongly constrained. Walker et al (1991) find that it must lie in the range

$$0.010\,h^{-2} < \Omega_b < 0.015\,h^{-2}, \tag{3.1}$$

where the upper and lower limits come from the upper bounds on ^{4}He and $^2\mathrm{D} + {}^3\mathrm{He}$, respectively. The upper limit implies that Ω_b is well below 1, which suggests that no baryonic candidate could provide the critical density required in the inflationay scenario. The standard scenario therefore assumes that the total density parameter is 1, with only the fraction given by (3.1) being baryonic. Until recently, cold inos seemed to be most compatible with large-scale structure observations; this led to the popularity of the CDM scenario.

Recently, X-ray data on the mass of gas in groups and clusters of galaxies suggest that the standard CDM picture may not be satisfactory. Although the gas does not suffice to explain all the dark matter, the ratio of the visible baryon mass (i.e. the mass in the form of stars and hot gas) to total mass is still anomalously high compared to the mean cosmic ratio implied by Equation (3.1). For example, the baryon fraction is 13% for the small group HCG62 (Ponman & Bertram 1993) and it tends to be in the range 20–30% for rich clusters. In particular, *ROSAT* observations of Coma suggest that the baryon fraction within the central 3 Mpc is about 25%, which is five times as large as the standard cosmological ratio (White et al 1993). It is hard to understand how the extra baryon concentration would come about since dissipation should be unimportant on these scales and most other astrophysical processes (such as winds and supernovae) should *decrease* the local baryon fraction. [See, however, Babul & Katz (1993) for a contrary view.] Unless one invokes a cosmological constant, this suggests that either the cosmological density is well below the critical value or the baryon density is much higher than implied by the standard cosmological nucleosynthesis scenario.

In the past few years considerable work has focused on the question of whether one can circumvent condition (3.1) by invoking a first-order phase transition at the quark-hadron era. The idea is that the transition would generate fluctuations in the baryon density. Neutrons would then diffuse from the overdense regions (because their cross-section is less than that of the protons), which would lead to variations in the neutron-to-proton ratio. One can then produce deuterium in the regions where the density is low, without appreciably modifying the average helium production (Applegate et al 1987, Alcock et al 1987). However, there is still a problem getting the observed lithium abundance. This arises because, as one varies Ω_b, $X(^7\mathrm{Li})$ has a minimum at around $\Omega_b \sim 0.01$, and the observed abundance almost exactly matches this minimum. Any fluctuations in the baryon density will therefore tend to lead to an overabundance of lithium.

Interest in the effects of the quark-hadron transition was revived by the suggestion of Malaney & Fowler (1988) that neutrons could diffuse back into the overdense regions and destroy lithium, provided that the separation between the nucleation sites was finely-tuned ($d \sim 10$ m). However, in this case, helium may be overproduced. A detailed numerical investigation of the effects of simultaneously varying Ω_b, d, the amplitude of the baryon density fluctuations (R), and the volume fraction at high density (f_v) by Kurki-Suonio et al (1990) suggested that, although values of R as large as 100 are compatible with observation if $d < 300$ m, one can never have $\Omega_b = 1$. More recently, Mathews et al (1993) have argued that the largest possible value for the baryon density is $\Omega_b = 0.09h^{-2}$, so a critical density of baryons still seems to be excluded unless $H_o < 35$. For an up-to-date review of inhomogeneous nucleosynthesis, see Malaney & Mathews (1993).

3.2 *Microwave Anisotropies*

A second argument for nonbaryonic dark matter is associated with the upper limits on and detections of anisotropies in the cosmic microwave background (CMB). To form the observed large-scale structure through purely gravitational processes, the amplitude of the fluctuations in the matter density at decoupling must have exceeded a minimum value; this implies a minimum amplitude for the CMB anisotropies which may contravene observations for a purely baryonic model. The anisotropies are reduced in a model dominated by nonbaryonic dark matter ($\Omega \gg \Omega_b$), partly because the density fluctuations start growing earlier (from when the dark matter dominates the density) and partly because they continue growing for a longer period (fluctuations freezing out at a redshift $z \approx \Omega^{-1}$). Despite this argument, it is not clear that the anisotropy constraints require Ω to be as large as 1—especially if one relinquishes scale-invariant fluctuations—because both the amplitude and angular scale of the anisotropies are reduced in a low density Universe owing to the effects of radiation pressure at decoupling (Coles & Ellis 1994). In the past few years, therefore, much attention has focused on baryon-dominated models with "primeval isocurvature" fluctuations (Peebles 1987a,b). The fluctuations are assumed to have a power-law form and the problem is to determine whether one can choose a spectral index n which simultaneously matches the *COBE* anisotropies at 10°–90° (Smoot et al 1992) and the large-scale structure data (Cen et al 1993). One can already place strong constraints on the combination of Ω_b and n (Efstathiou et al 1992, Gouda & Sugiyama 1992), and some researchers claim that baryon-dominated models are already excluded (Chiba et al 1993).

3.3 *Arguments for Baryonic Dark Matter*

The cosmological nucleosynthesis argument is a two-edged sword: It requires both baryonic and nonbaryonic dark matter (Pagel 1990). This is because the value of Ω_b allowed by Equation (3.1) almost certainly exceeds the density of visible baryons Ω_v. A careful inventory by Persic & Salucci (1992) shows that the contributions to Ω_v are 0.0007 in spirals, 0.0015 in ellipticals and spheroidals, $0.00035\,h^{-1.5}$ in hot gas within an Abell radius for rich clusters, and $0.00026\,h^{-1.5}$ in hot gas out to a virialization radius in groups and poor clusters. This gives a total of $(2.2+0.6\,h^{-1.5}) \times 10^{-3}$, so Equation (3.1) implies that the fraction of baryons in dark form must be in the range 70%–95% for $0.5 < h < 1$. Note, however, that the Persic-Salucci estimate does not include any contribution from low surface brighteners galaxies (McGaugh 1994) or dwarf galaxies (Bristow & Phillipps 1994).

The discrepancy between Ω_b and Ω_v could be resolved if there were an appreciable density of intergalactic gas. We know there must be some neutral gas in the form of Lyman-α clouds, but the density parameter associated with the "damped" clouds is probably no more than $0.003\,h^{-2}$ (Lanzetta et al 1991)—comparable to the density in galaxies, and consistent with the idea that these are protogalactic disks. Although the missing baryons could conceivably be in the form of a hot intergalactic medium (either never incorporated into galaxies or expelled by supernovae and galactic winds), the temperature would need to be finely tuned (Barcons et al 1991). The Gunn-Peterson test requires $\Omega(\text{HI}) < 10^{-8}h^{-1}$ (Sargent & Steidel 1990), while the *COBE* limit on the Compton distortion of the microwave background ($y < 3 \times 10^{-5}$) requires that, for a temperature T at redshift z,

$$\Omega(\mathrm{HII}) < 0.03 \left(\frac{T}{10^8\mathrm{K}}\right)^{-1} \left(\frac{y}{10^{-5}}\right) [(1+z)^{3/2} - 1]^{-1} h^{-1}\mathrm{K} \tag{3.2}$$

(Mather et al 1994). The latter limit implies that a smooth intergalactic medium (IGM) cannot generate the observed X-ray background, although there is still a temperature range beween 10^4 K and 10^8 K in which one could have $\Omega_{\mathrm{IGM}} \sim \Omega_{\mathrm{b}}$. Whether one could *expect* so much gas to remain outside galaxies depends on its thermal history (Blanchard et al 1992).

The other possibility is that the missing baryons are inside galactic halos. The halo dark matter cannot be in the form of hot gas for it would generate too many X rays. Recently, however, Pfenniger et al (1993) have argued that it could be in the form of cold molecular gas. In their model, the gas is initially in the form of dense cloudlets with mass $10^{-3} M_{\odot}$ and size 30 AU in a rotationally supported disk. The cloudlets then build up fractally to larger scales. Their model is motivated by the claim that spirals evolve along the Hubble sequence from Sd to Sa and that their mass-to-light ratio decreases in the process, which requires that the dark matter be progressively turned into stars. It also explains why the surface density ratio of dark matter and HI gas is constant outside the optical disk (Carignan et al 1990).

The final possibility—and the one that is the focus of the rest of this review—is that the dark baryons have been processed into stellar remnants. Even if stellar remnants have enough density to explain the alleged dark matter in the Galactic disk, this would be well below the value required by Equation (3.1), for if all disks have the 60% dark component envisaged for our Galaxy by Bahcall et al (1992a), this only corresponds to $\Omega_{\mathrm{v}} \approx 0.001$. The more interesting question is whether the baryonic density could suffice to explain the dark matter in galactic halos; the term "Massive Compact Halo Object" or "MACHO" has been coined in this context. If our Galaxy is typical, the density associated with galactic halos would be $\Omega_{\mathrm{h}} \approx 0.01\mathrm{h}^{-1}(R_{\mathrm{h}}/35\ \mathrm{kpc})$ where R_{h} is the halo radius. [The mass-to-light ratio for our Galaxy is (14–24) ($R_{\mathrm{h}}/35$ kpc) (Fich & Tremaine 1991) corresponding to $\Omega_{\mathrm{h}} = (0.008\text{–}0.014)h^{-1}(R_{\mathrm{h}}/35\ \mathrm{kpc})$; a more precise calculation would involve integrating over galaxies of all masses but then one would need to know the mass-dependence of R_{h} (Ashman et al 1993).] Thus Equation (3.1) implies that *all* the dark matter in our halo could be baryonic only for $R_{\mathrm{h}} < 50\,h^{-1}$kpc. We saw in Section 2.2 that the minimum size of our halo is 70 kpc, which would just be compatible with this. If it is larger, the baryonic fraction could only be $(R_{\mathrm{h}}/50\,h^{-1}\mathrm{kpc})^{-1}$. The cluster dark matter has a density $\Omega_{\mathrm{c}} \approx 0.1$ and Equation (3.1) implies that this matter cannot be purely baryonic unless one invokes inhomogeneous nucleosynthesis.

We note that there is no necessity for the Population III stars to form before galaxies just as long as some change in the conditions of star formation makes their mass different from what it is today. However, the epoch of formation will be very important for the relative distribution of baryonic and nonbaryonic dark matter, especially if the nonbaryonic dark matter is "cold" so that it can cluster in galactic halos. In this case, if the Population III stars form before galaxies, one might expect their remnants to be distributed throughout the Universe (White & Rees 1978), with the ratio of the baryonic and nonbaryonic densities being the same everywhere and of order 10. If they form at the same time as galaxy formation, perhaps in the first phase of protogalactic collapse, one would expect the remnants to be confined to halos and clusters. In this case, their contribution to the halo density could be larger since the baryons would probably dissipate and become more concentrated. Angular momentum considerations suggest that the local baryon fraction must be increased by at least a factor of 10 (Fall & Efstathiou 1981). If the WIMPs are hot and cannot cluster in halos, then halos would consist exclusively of MACHOs. These possibilities are illustrated in Figure 1.

3.4 *Variants of the Baryonic Dark Matter Scenario*

One may consider three variants of Baryonic Dark Matter (BDM) scenario, depending on how strongly one wishes to retain homogeneous primordial nu-

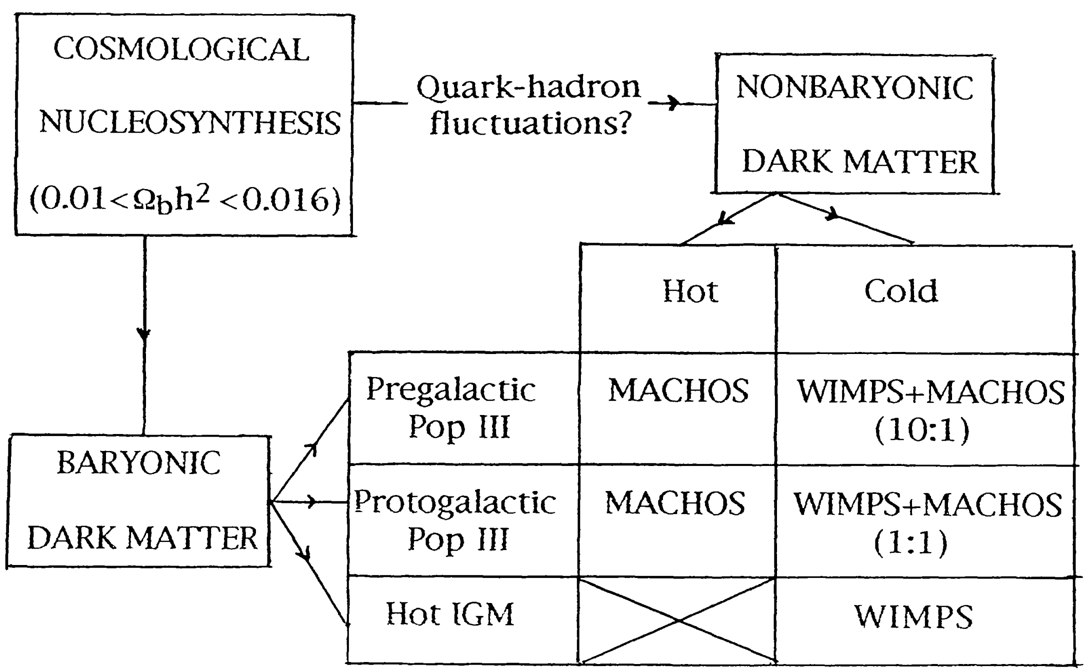

Figure 1 The relative contributions of WIMPs and MACHOs to the halo density in various scenarios. Halos can consist exclusively of WIMPs only if the dark baryons are in a hot intergalactic medium and they can consist exclusively of MACHOs only if the WIMPs are hot. The most natural hypothesis is that they contain both.

cleosynthesis, inflation, and nonbaryonic dark matter:

- In the *standard* BDM scenario, one retains all three assumptions, which requires $\Omega_b \approx 0.01\,h^{-2}$ and $\Omega = 1$. In this case, we conclude that 70% to 95% of baryons are dark but MACHOs alone can provide galactic halos only if $R_h < 50\,h^{-1}$kpc. The cluster and critical density dark matter must be WIMPs and, if they are cold, the halo dark matter is expected to be a mixure of MACHOS and WIMPS. This conclusion pertains even for $\Omega < 1$, as may be required by the large baryon fraction in clusters.

- In the *maximal* BDM scenario, one assumes that the Universe has a critical density of baryons ($\Omega_B = \Omega = 1$), thereby relinquishing the need for nonbaryonic dark matter without giving up inflation (Fowler 1990). The scenario is inconsistent with homogeneous nucleosynthesis unless one invokes unrealistically low values of H_o. When the upper limit on Ω_b was $0.06\,h^{-2}$ s (Yang et al 1984), it was possible to have $\Omega_b = 1$ by invoking the only moderately extreme value $H_o = 25$ (Shanks 1985), but the new upper limit would require $H_o = 10$, which is probably absurd [see, however, Harrison (1993) for a contrary view].

- In the *baryon-dominated* scenario, one only assumes the existence of the dark matter for which there is direct dynamical evidence and attributes this solely to baryons ($\Omega_b = \Omega \approx 0.1$). In this case, one has to give up both inflation and homogeneous nucleosynthesis. In order to explain the observed light element abundances, one then has to invoke some exotic astrophysical process, such as the spallation of primordial helium by high energy photons from accreting black holes (Gnedin & Ostriker 1992). The viability of this scenario also depends on whether the isocurvature baryon-dominated model is compatible with the CMB anisotropy constraints.

Most of the emphasis in this review is on the standard BDM scenario but, in assessing which baryonic candidates are viable, it is important to bear in mind the more radical proposals.

4. POPULATION III STARS

There is some confusion in the literature because the term "Population III" has been used in two distinct contexts. It has been applied to describe: 1. the stars that generate the first metals; and 2. the stars hypothesized to provide the dark matter in galactic halos. In either case, the stars only warrant a special name if they are definitely distinct from Population II stars, i.e. if they form at a distinct epoch or if the initial mass function (IMF) of the first stars is bimodal (with distinct populations of stars forming in different locations). We will see that this may not be the case for stars of type 1, but it probably is for stars of type

2. If one requires *both* kinds of "Population III" stars, it is not obvious which ones come first. One could envisage situations in which the dark objects form before, after, or contemporaneously with the stars that make the first metals.

4.1 *Population III as the First Metal Producers*

Stars of type 1 must exist because heavy elements can only be generated through stellar nucleosynthesis. However, the most natural assumption is that these are merely the ones at the high mass end of the Population II mass spectrum, since in this case they would generate the first metals because they evolved fastest. This is already sufficient to explain most of the abundance characteristics of Population I and II stars (Truran 1984, Wheeler et al 1989, Rana 1991, Pagel 1992). At one point, there appeared to be a metallicity cut-off of order 10^{-5} below which no stars were found (Bond 1981); this suggested that the first stars were more massive than those forming today. However, the evidence for the cut-off has now gone away: Beers et al (1992) find that the Z distribution for Population II stars extends well below 10^{-6}, and there exists one object with $Z = 6 \times 10^{-7}$ (Bessel & Norris 1984). In any case, the number of low-Z objects is not necessarily incompatible with the assumption that the IMF has always been the same (Pagel 1987), so there is no obvious reason for supposing that the first stars were qualitatively different from Population II. However, one cannot be sure that there are not abundance anomalies at some level (cf Kajino et al 1990, Suntzeff 1992). This is important because, if the dark baryons are in the remnants of massive stars, one might expect some nucleosynthetic consequences.

4.2 *Population III as Dark Matter Producers*

We have seen that it is possible that most of the baryons were processed through a first generation of pregalactic or protogalactic stars and henceforth the term "Population III" is used specifically in this sense. However, it should be stressed that the cosmological interest in Population III stars is not confined to the dark matter issue. They would also be expected to produce radiation, explosions, and nucleosynthesis products, and each of these could have important cosmological consequences (Carr et al 1984). Although there are no observations which unambiguously *demand* that most of the baryons were processed through Population III stars, there are theoretical reasons for anticipating their formation. This is because the existence of galaxies and clusters of galaxies implies that there must have been density fluctuations in the early Universe and, in many scenarios, these fluctuations would also give rise to a population of pregalactic stars. The precise way in which this occurs depends on the nature of the fluctuations and the nature of the dominant dark matter, as we now discuss.

In a baryon-dominated universe with isothermal or isocurvature density fluctuations, the first bound objects usually have a mass corresponding to the baryonic Jeans mass at decoupling. This is $M_{Jb} \approx 10^6 \Omega_b^{-1/2} M_{\odot}$, where Ω_b is the baryon density parameter, and clouds of this mass would bind at a redshift ~100, depending on the form of the spectrum of fluctuations at decoupling. Larger bound objects—like galaxies and clusters of galaxies—would then build up through a process of hierarchical clustering (Peebles & Dicke 1968). Regions smaller than M_{Jb}, even though their initial overdensity might be higher, would not begin to collapse until they were larger than the Jeans length and by then they would generally have been erased either by viscous damping prior to decoupling or by nonlinear processes during the oscillatory period after decoupling (Carr & Rees 1984). However, more exotic possibilities arise if the fluctuation spectrum is sufficiently steep for the fluctuations to be *highly* nonlinear on smaller scales because, in this case, very small regions could collapse well before recombination (Hogan 1978). Indeed, this is expected in the primordial isocurvature baryon-dominated model (Hogan 1993).

In the Cold Dark Matter scenario, in which the density of the Universe is dominated by cold particle relics, structure also builds up hierarchically (Blumenthal et al 1984). In this case, one expects bound clumps of the particles to form down to very small scales (Hogan & Rees 1988), but baryons would only fall into the potential wells, forming bound clouds, on baryon scales above $M_{Ja} \approx 10^6 \Omega_b \Omega_a^{-3/2} M_{\odot}$, where Ω_a is the cold particle density (Carr & Rees 1984, de Araujo & Opher 1990). In fact, the formation of the pregalactic clouds is even easier in this case because the cold particle fluctuations grow by an extra factor of $10\Omega_a$ between the time when the cold particles dominate the density and decoupling.

In a baryon-dominated universe with adiabatic density fluctuations, the first objects to form are pancakes of cluster size (Zeldovich 1970) because adiabatic fluctuations are erased by photon diffusion for $M < 10^{13} \Omega_b^{-5/4} M_{\odot}$ (Silk 1968). Galaxies and smaller scale structures therefore have to form as a result of fragmentation. This scenario appears to be excluded by CMB anistropy constraints but a similar picture applies if one has adiabatic fluctuations in a Hot Dark Matter scenario, in which the Universe's mass is dominated by a particle like the neutrino. In this case, the fluctuations are erased by neutrino free-streaming for $M < 10^{15} \Omega_\nu^{-2} M_{\odot}$ (Bond et al 1980), so the first objects to form are pancakes of supercluster scale. In both scenarios one expects the pancakes to initially fragment into clumps of mass $10^8 M_{\odot}$; these clumps must then cluster in order to form galaxies. Even in this case, therefore, one might expect pregalactic clouds to form, albeit at a relatively low redshift ($z < 10$).

All of these scenarios would be modified if the Universe contained topological relics such as strings or textures (Cen et al 1991). Such relics could induce the formation of smaller scale bound regions than usual. For example, Silk & Stebbins (1993) find that in the CDM picture with strings, up to 10^{-3} of the mass of the Universe could go into cold dark matter clumps at the time of matter-radiation equilibrium. These clumps would then accrete baryonic halos, forming globular-cluster type objects.

In the explosion scenario (Ostriker & Cowie 1981, Ikeuchi 1981), the first objects to form are explosive seeds (stars or clusters of stars). These generate shocks which sweep up vast shells of gas; when the shells overlap, most of the gas gets compressed into thin sheets (Carr & Ikeuchi 1985). The sheets then fragment either directly into galaxies or into lower-mass systems, depending on the cooling mechanism (Bertschinger 1983, Wandel 1985). Although the explosion scenario was originally invoked to explain large-scale structure, this now seems to be incompatible with the upper limit on the y-parameter permitted by *FIRAS*. However, one can still envisage this as a mechanism for amplifying the fraction of the gas going into stars—an idea applicable in models with or without nonbaryonic dark matter (Scherrer 1993).

4.3 *Expected Mass of Population III Stars*

In all these scenarios, an appreciable fraction of the Universe may go into subgalactic clouds before galaxies themselves form. What happens to these clouds? In some circumstances, one expects them to be disrupted by collisions with other clouds because the cooling time is too long for them to collapse before coalescing. However, there is usually some mass range in which the clouds survive. For example, the range is 10^6–$10^{11} M_\odot$ in the hierarchical clustering scenario. In this case, they could face various possible fates. They might just turn into ordinary stars and form objects like globular clusters. On the other hand, the conditions of star formation could have been very different at early times and several alternatives have been suggested.

Some people argue that the first stars could have been much smaller than at present. Fairly general arguments suggest that the minimum fragment mass could be as low as 0.007 $M_\odot$ (Low & Lynden-Bell 1976, Rees 1976) and it is possible that conditions at early epochs—such as the enhanced formation of molecular hydrogen (Palla et al 1983, Yoshii & Saio 1986, Silk 1992)—could allow the formation of even smaller objects. One might also invoke the prevalence of high-pressure pregalactic cooling flows (Ashman & Carr 1988, Thomas & Fabian 1990), analagous to the cluster flows observed at the present epoch (Fabian et al 1984) but on a smaller scale. This possibility is discussed in detail in Section 9.2.

Other people argue that the first stars could have been much larger than at present. For example, the fragment mass could be increased before metals formed because cooling would be less efficient (Silk 1977). There is also observational evidence that the IMF may become shallower as metallicity decreases (Terlevich 1985), thereby increasing the fraction of high mass stars. Another possibility is that the characteristic fragment mass could be increased by the effects of the microwave background (Kashlinsky & Rees 1983) or by the absence of substructure in the first bound clouds (Tohline 1980).

One could also get a mixture of small and large stars. For example, Cayrel (1987) has proposed that one gets the formation of massive exploding stars in the core of the cloud, followed by the formation of low mass stars where the gas swept up by the explosions encounters infalling gas. Kashlinsky & Rees (1983) have proposed a scheme in which angular momentum effects lead to a disk of small stars around a central very massive star. Salpeter & Wasserman (1993) have a scenario in which one gets clusters of neutron stars and asteroids.

In the baryon-dominated isocurvature scenario, with highly nonlinear fluctuations on small scales, the collapse of the first overdense clouds depends on the effects of radiation diffusion and trapping. Hogan (1993) finds that sufficiently dense clouds collapse very early into black holes with a mass of at least $1 M_{\odot}$, while clouds below this critical density delay their collapse until after recombination and may produce neutron star or brown dwarf remnants. One of the attractions of this idea is that it allows a baryon density parameter higher than that indicated by Equation (3.1) because the nucleosynthetic products in the high density regions are locked up in the remnants, leaving the products from the low density regions outside (cf Gnedin et al 1994).

It is possible that the first clouds collapse directly to form supermassive black holes (Gnedin & Ostriker 1992). Usually clouds will be tidally spun up by their neighbors as they become gravitationally bound and the associated centrifugal effects then prevent direct collapse. However, just after recombination, Compton drag could prevent this tidal spin-up, especially if the gas becomes ionized or contains dust (Loeb 1993). More detailed numerical hydrodynamical studies of this situation have been presented by Umemura et al (1993), who allow for different ionization histories and for different ratios of baryonic to nonbaryonic density. For a fully ionized gas, the baryonic disk loses angular momentum very effectively and shrinks adiabatically. Even if rotation is important, one could still get a supermassive disk which slowly shrinks to form a black hole due to angular momentum transport by viscous effects (Loeb & Rasio 1993). One might even end up with a supermassive binary system.

While there is clearly considerable uncertainty as to the fate of the first bound clouds, our discussion indicates that they are likely to fragment into stars that are either larger or smaller than the ones forming today. Theorists merely disagree about the direction! One certainly needs the stars to be very different if they are to produce a lot of dark matter. One also requires the clouds to fragment very efficiently. Although this might seem rather unlikely, there are circumstances even in the present epoch where this occurs; for example, in starburst galaxies or cooling flows. This is also a natural outcome of the hierarchical explosion scenario (Carr & Ikeuchi 1985).

We note that there is no necessity for the Population III stars to form before galaxies. It is possible that the Population III clouds just remain in purely gaseous form and become Lyman-α clouds (Rees 1986), in which case the formation of the dark-matter-producing stars would need to be postponed until the epoch of galaxy formation. Nevertheless, there is at least the possibility that the Population III stars were pregalactic, and this would have various attractions. For example, it would permit the Universe to be reionized at high redshifts (Hartquist & Cameron 1977), thereby hiding small-scale anisotropies in the microwave background (Gouda & Sugiyama 1992), and it might help to explain why the intergalactic medium appears to be ionized back to redshifts of at least 5 (Schneider et al 1991). Pregalactic stars might also be invoked to explain pregalactic enrichment (Truran & Cameron 1971) and the existence of substantial heavy element abundances in intergalactic clouds at redshifts above 3 (Steidel & Sargent 1988) and in intracluster gas at low redshifts (Hatsukade 1989).

4.4 *Population III Remnants*

Even if a large fraction of the baryons are processed through Population III stars, this does not necessarily guarantee dark matter production. However, most stars ultimately produce dark remnants and we now list the various possibilities.

LOW MASS OBJECTS We will see in Section 9.3 that stars in the range 0.08–0.8 $M_\odot$ (which are still on the main-sequence) are probably excluded from explaining any of the dark matter problems. However, objects in the range 0.001–0.08 $M_\odot$ would never burn hydrogen and would certainly be dim enough to escape detection. [Note that Salpeter (1993) argues that the critical mass for hydrogen burning could be higher for Population III stars because slow protostellar accretion could lead to degenerate cores with lower central temperatures than usual.] Such brown dwarfs (BDs) represent a balance between gravity and degeneracy pressure. Those above 0.01 $M_\odot$ could still burn deuterium; Shu et al (1987) have argued that this may represent a lower limit to a BD's mass but this conclusion is not definite. The evidence for stars in the brown dwarf mass range (e.g. Simon & Becklin 1992, Steele et al 1993) is controversial, but this merely reflects the fact that they are hard to find (Stevenson 1991) and it would be very surprising if the IMF happened to cut off just above $0.08 M_\odot$. Most searches have focused on BDs in binary systems with M-dwarfs; however, we already know that the BDs making up the dark matter could not be in such binaries else the M-dwarfs would have more than the dark density (cf McDonald & Clarke 1993). Objects below $0.001 M_\odot$ are held together by intermolecular rather than gravitational forces (i.e. they have atomic density) and may be described as snowballs. We will see in Section 10.1 that such objects are unlikely to constitute the dark matter.

INTERMEDIATE MASS OBJECTS Stars in the range 0.8–4 $M_\odot$ would leave white dwarf remnants, while those between $8M_\odot$ and some mass $M_{\rm BH}$ would leave neutron stars remnants. In either case, the remnants would eventually cool and become dark. (Stars in the mass range 4–8 $M_\odot$ could be disrupted entirely during their carbon-burning stage.) Stars more massive than $M_{\rm BH}$ could evolve to black holes; the value of $M_{\rm BH}$ is uncertain but it may be as high as $50M_\odot$ (Schild & Maeder 1985) or as low as $25M_\odot$ (Maeder 1992). Only intermediate mass remnants definitely form at the present epoch; this is why some theorists favor them as dark matter candidates (Silk 1991, 1992, 1993). However, we will see in Section 5.2 that their nucleosynthetic consequences may make them poor dark matter candidates.

VERY MASSIVE OBJECTS Stars in the mass range above 100 $M_\odot$, which are termed "Very Massive Objects" or VMOs, would experience the pair-instability during their oxygen-burning phase (Fowler & Hoyle 1964). This would lead to disruption below some mass M_c but complete collapse above it (Woosley & Weaver 1982, Ober et al 1983, Bond et al 1984). VMO black holes may therefore be more plausible dark matter candidates than ordinary stellar black holes. In the absence of rotation, $M_c \approx 200M_\odot$; however, M_c could be as high as $2 \times 10^4 M_\odot$ if rotation were maximal (Glatzel et al 1985). Note that stars with an initial mass above 100 $M_\odot$ are radiation-dominated and therefore unstable to pulsations during hydrogen burning. These pulsations would lead to considerable mass loss but are unlikely to be completely disruptive. Nevertheless, there is no evidence that VMOs form at the present epoch, so they are invoked specifically to explain dark matter.

SUPERMASSIVE OBJECTS Stars larger than $10^5 M_\odot$ are termed "Supermassive Objects" or SMOs. If they are metal-free, they would collapse directly to black holes on a timescale $10^4(M/10^5 M_\odot)^{-1} y$ before any nuclear burning (Fowler 1966). They would therefore have no nucleosynthetic consequences, although they could explode in some mass range above $10^5 M_\odot$ if they had nonzero metallicity (Fricke 1973, Fuller et al 1986). SMOs would also generate very little radiation, emitting only 10^{-11} of their rest-mass energy in photons. The existence of SMOs is rather less speculative than that of VMOs since supermassive black holes are thought to reside in some galactic nuclei and to power quasars (Blandford & Rees 1991). However, these would only have a tiny cosmological density.

Note that Population III stars are likely to span a range of masses, so the remnants need not be confined to one of the candidates listed above. From the point of view of the dark matter problem, one is mainly interested in where *most* of the mass resides. However, the other components could also have important observational consequences, as in the Salpeter & Wasserman (1993) scenario,

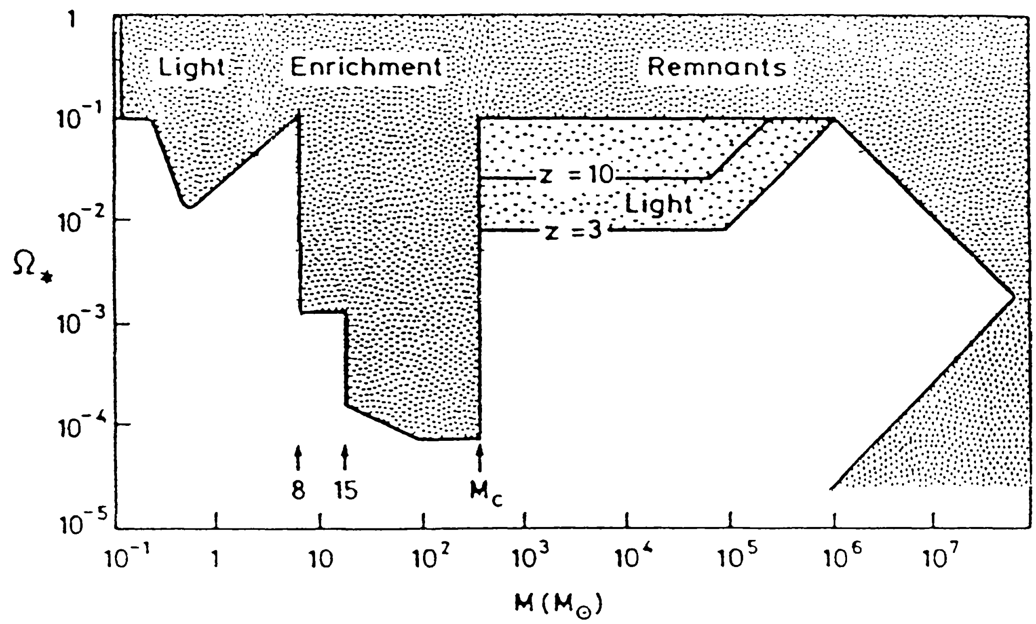

Figure 2 Summary of the various constraints on the density of Population III stars of mass M (an updated version of Figure 6 in Carr et al 1984). All the limits except the "light" one assume that the objects are inside galactic halos. The light limit is only interesting for stars that burn at $z < 30$ unless the light is reprocessed by dust. The nucleosynthesis limits for $M > 10^2 M_\odot$ assume that the fraction of mass lost during the hydrogen and helium burning phase is not too large.

where the small number of neutron stars is invoked to explain gamma-ray bursts.

5. CONSTRAINTS ON POPULATION III

In this section we review the constraints that can be placed on Population III stars and their remnants by considering their generation of background light and nucleosynthetic products. The discussion is only brief because these limits are essentially the same as they were a decade ago. The constraints on $\Omega_*(M)$, the density of stars of mass M in units of the critical density, are summarized in Figure 2, which is an updated version of Figure 6 from Carr et al (1984). The remnant constraints, which are also shown in Figure 2, are discussed in detail in Section 6.

5.1 *Background Light Constraints*

An effect that constrains the number of Population III objects over every mass range between 0.1 and $10^5 M_\odot$ is the generation of background light during the stellar main-sequence phase. The fact that the observed background radiation density over all wavebands cannot exceed $\Omega_{RO} \approx 10^{-4}$ in units of the critical density (and it is smaller in most bands) permits a general constraint on $\Omega_*(M)$. One can obtain more precise constraints by using information about the waveband in which the radiation is expected to reside (Peebles & Partridge 1967, Thorstensen & Partridge 1975, Carr et al 1984, McDowell 1986, Negroponte 1986) but an integrated background light limit has the virtue of generality.

For stars larger than $0.8\,M_\odot$, which have already burnt their nuclear fuel, one just compares their total light production to Ω_{RO} to obtain a constraint on $\Omega_*(M)$. Since 7 MeV per baryon is released in burning hydrogen to helium, the background light density generated should be $\Omega_R = 0.007\,\Omega_* f_b(1+z_*)^{-1}$ in units of the critical density, where z_* is the redshift at which the stars burn their fuel (the minimum of the formation redshift z_f and the redshift z_{MS} at which the age of the Universe equals their main-sequence time) and f_b is the fraction of the star's mass burnt into helium. By using the known dependence of f_b and z_{MS} on M, one can predict the value of Ω_R as a function of Ω_*, M, and z_f. Since the observed background density over all wavebands does not exceed 10^{-4}, this implies a constraint on Ω_* as function of M and z_f. For stars with $M < 0.8\,M_\odot$, which are still burning, one compares the product of the luminosity $L(M)$ and the age of the Universe to Ω_{RO}. The resulting constraints on $\Omega_*(M, z_*)$ are shown in Figure 2; these are somewhat stronger than indicated by Carr et al (1984) because the limits on Ω_{RO} have improved (See Section 6.1). Peebles & Partridge (1967) used this argument to preclude stars in the mass range 0.3–$2.5 M_\odot$ from having the critical density.

5.2 *Enrichment Constraints*

One of the strongest constraints on the spectrum of Population III stars comes from the fact that stars in the mass range $4M_\odot$ to $M_c \approx 200M_\odot$ should produce an appreciable heavy element yield (Arnett 1978), either via winds in their main-sequence phase or during their final supernova phase. We take the yield Z_{ej} to be 0.01 for $8\,M_\odot < M < 15\,M_\odot$, $0.5-(M/6\,M_\odot)^{-1}$ for $15\,M_\odot < M < 100\,M_\odot$, and 0.5 for $100\,M_\odot < M < M_c$ (Wheeler et al 1989). Carr et al (1984) took $z_{ej} = 0.2$ for $4M_\odot < M < 8M_\odot$ on the assumption that such stars explode as a result of degenerate carbon burning. However, it seems possible that they evolve to white dwarfs without exploding, so Figure 2 assumes there is no enrichment for $M < 8M_\odot$. Whether Population III stars are pregalactic or protogalactic, the enrichment they produce cannot exceed the lowest metallicity observed in Population I stars ($Z = 10^{-3}$). One infers that the density of the stars must satisfy

$$\Omega_* < 10^{-3} Z_{ej}^{-1} \Omega_g = 10^{-4} \left(\frac{Z_{ej}}{0.1}\right)^{-1} \left(\frac{\Omega_g}{0.01}\right), \qquad (5.1)$$

where Ω_g is the gas density before the stars form, assumed to be around 0.01

in view of the Equation (3.1). This enrichment constraint is shown in Figure 2 [note that it is stronger than indicated by Carr et al (1984) because they assumed $\Omega_g = 0.1$.] It immediately excludes neutron stars or ordinary stellar black holes from explaining any of the dark matter problems unless the Population III precursors are clumped into clusters whose gravitational potential is so high that ejected heavy elements cannot escape (Salpeter & Wasserman 1993). If one wants to produce the dark matter without contravening the enrichment constraint, the most straightforward solution is to assume that the spectrum either starts above M_c (as in the black hole scenario) or ends below $8M_\odot$ (as in the brown dwarf or white dwarf scenario), so that there is no pregalactic enrichment at all.

5.3 *Helium Constraints*

Although stars return helium to the background Universe in most mass ranges, the associated constraints on the fraction of the Universe going into Population III stars are only weak because of the uncertainties in the primordial helium abundance. However, the helium limit is important in the $M > M_c$ range because there may be no heavy element yield here. Because the pulsational instability leads to mass-shedding of material convected from its core, a VMO is expected to return helium to the background medium during core-hydrogen burning (Bond et al 1983). The net yield depends sensitively on the mass loss fraction ϕ_L. If this is very high, the yield will be low because most of the mass will be lost before significant core burning occurs. However, for ϕ_L below the critical value $(1 - Y_i)/(2 - Y_i)$, the mass loss is always slower than the shrinkage of the convective core and one can show that the fraction of mass returned as new helium is

$$\Delta Y = \left(1 - \frac{Y_i}{2}\right)\phi_L^2 \leq 0.25(1 - Y_i)^2 \left(1 - \frac{Y_i}{2}\right)^{-1} \quad (5.2)$$

Here Y_i is the initial (primordial) helium abundance and the equality sign on the right applies only if ϕ_L has the critical value. This does not impose a useful constraint on the number of VMOs if ϕ_L is well below the critical value since ΔY is then very small. However, there is some indication from numerical calculations that hydrogen-shell burning may produce a super-Eddington luminosity which completely ejects the stellar envelope (Woosley & Weaver 1982, Bond et al 1984). This would guarantee the maximal helium production permitted by Equation (5.2) and have profound cosmological implications. If $Y_i = 0.23$, corresponding to the conventional primordial value, $\Delta Y = 0.17$, so one would substantially overproduce helium if much of the Universe went into VMOs. In this case, only black holes in the mass range above $10^5 M_\odot$ could be viable candidates for the dark matter. On the other hand, if $Y_i = 0$, then $\Delta Y = 0.25$, which is tantalizingly close to the standard primordial value. This raises the question of whether the Population III VMOs invoked to produce the dark matter might also generate the helium usually attributed to cosmological nucleosynthesis. Of course, the added attraction of the hot Big Bang model is that it predicts the observed abundances of other light elements. One might conceivably generate these elements by invoking high energy photons from accreting black holes to spallate helium—either within the surrounding accretion tori (Rees 1984, Ramadurai & Rees 1985; Jin 1989, 1990) or in the background Universe (Gnedin & Ostriker 1992, Gnedin et al 1994); however, these models seem somewhat contrived.

5.4 *Black Hole Accretion Constraints*

Any black hole remnants of Population III stars would tend to generate radiation through accretion; this could be important at both the present and pregalactic epochs. In particular, if we assume that halo or disk black holes accrete ambient gas at the Bondi rate and that the accreted material is converted into radiation with efficiency η, then one may impose interesting constraints on the density of the black holes $\Omega_B(M)$ merely by requiring that the radiation density generated since the epoch of galaxy formation does not exceed the observed density in the appropriate waveband. For example, if we assume that the radiation emerges at 10 keV and that $\eta = 0.1$, we infer $\Omega_B(M) < (M/10^5 M_\odot)^{-1}$ for halo holes and $\Omega_B(M) < (M)/10M_\odot)^{-1}$ for disk holes (Carr 1979). These limits have also been studied by Hegyi et al (1986). Stronger limits may come from constraints on the number of *individual* sources in our own Galaxy. Thus Ipser & Price (1977), using a particular accretion model, preclude $10^5 M_\odot$ holes from comprising the halo because of the non-observation of suitable infrared and optical sources.

One might expect the background light constraints to be even stronger for pregalactic black holes since the background gas density would have been higher at early times. If we assume Bondi accretion, then the luminosity will exceed the Eddington value for some period after decoupling if $M > 10^3 \eta^{-1} M_\odot$. However, the pregalactic limit is actually weaker: It takes the form $\Omega_B(M) < (M/10^6 M_\odot)^{-1}$ for $\eta = 0.1$ with only a weak dependence on the photon energy (Carr 1979). This is a consequence of two factors: 1. a large fraction of the emitted radiation goes into heating the matter content of the Universe rather than into background light; and 2. the heating of the Universe will boost the matter temperature well above the usual Friedmann value and this will reduce the accretion rate (Meszaros 1975, Carr 1981a, Gnedin & Ostriker 1992). Nevertheless, the effect on the thermal history of the Universe could be of great interest in its own right. For example, accreting black holes could easily keep the Universe ionized throughout the period after decoupling. The sort of background generated by the pregalactic accretion phase of a population of $10^6 M_\odot$ black holes is indicated in Figure 6.

6. DYNAMICAL CONSTRAINTS

A variety of constraints can be placed on the mass of any dark compact objects in the disk and halo of our own Galaxy by considering their dynamical effects. The constraints are usually calculated on the assumption that the objects are black holes but, as emphasized in Section 6.4, most of them also apply for dark clusters of smaller objects. There are also constraints for dark objects in clusters of galaxies or in the intergalactic medium, though these are weaker. The limits are summarized as upper limits on the density parameter $\Omega_B(M)$ for black holes of mass M in Figure 3, where the disk, halo, and cluster dark matter are assumed to have densities of 0.001, 0.1, and 0.2, respectively. Figure 3 updates and—in some respects corrects—Figure 1 of Carr (1978).

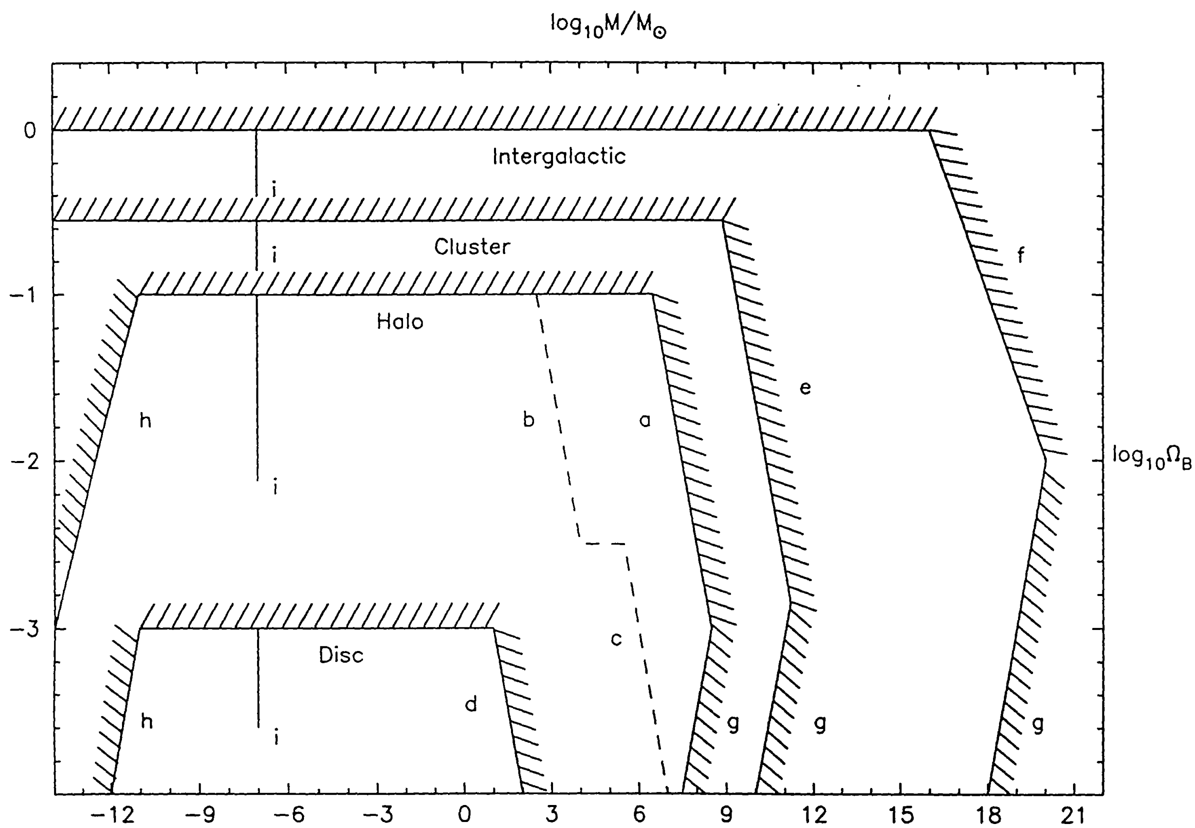

Figure 3 A summary of the dynamical constraints on the density parameter Ω_B for black holes of mass M located in the Galactic disk, the Galactic halo, clusters of galaxies, and the intergalactic medium. The total dark matter density in these cases is taken to be 0.001, 0.1, 0.2, and 1, respectively. The limits come from : (*a*) disk heating; (*b*) globular cluster disruption; (*c*) dynamical friction; (*d*) binary disruption; (*e*) galaxy distortions; (*f*) galaxy peculiar velocities; (*g*) one black hole per disk/halo/cluster/Universe; and (*h*) comet observations. Limits (*b*) and (*c*) are shown by broken lines because they are not so secure. The evaporation limit (*i*) is nondynamical.

6.1 *Disk Heating by Halo Holes*

As halo objects traverse the Galactic disk, they will impart energy to the stars there. This will lead to a gradual puffing up of the disk, with older stars being heated more than younger ones. Lacey & Ostriker (1985) have argued that black holes of around $10^6 M_\odot$ could provide the best mechanism for generating the observed amount of puffing. In particular, this explains: 1. why the velocity dispersion of the disk stars, σ, scales with age as $t^{1/2}$; 2. the relative velocity dispersions in the radial, azimuthal, and vertical directions; and 3. the existence of a high energy tail of stars with large velocity (Ipser & Semenzato 1985). In order to normalize the $\sigma(t)$ relationship correctly, the number density of the holes n must satisfy $nM^2 \approx 3 \times 10^4 M_\odot^2 \mathrm{pc}^{-3}$. Combining this with the local halo density $\rho_\mathrm{h} = nM \approx 0.01 M_\odot \mathrm{pc}^{-3}$ gives $M = 2 \times 10^6 M_\odot$.

This argument is no longer compelling because more recent measurements give smaller velocity dispersions for older stars, so that σ may no longer rise as fast as $t^{1/2}$ (Carlberg et al 1985, Stromgren 1987, Gomez et al 1990). Heating by a combination of spiral density waves and giant molecular clouds may now give a better fit to the data (Lacey 1991). Nevertheless, one can still use the Lacey-Ostriker argument to place an upper limit on the density in halo objects of mass M (Carr et al 1984):

$$\Omega_\mathrm{B} < \Omega_\mathrm{h} \min\left[1, \left(\frac{M}{M_\mathrm{heat}}\right)^{-1}\right], \qquad M_\mathrm{heat} = 3 \times 10^6 \left(\frac{t_\mathrm{g}}{10^{10} y}\right)^{-1}, \qquad (6.1)$$

where t_g is the age of the Galaxy. Otherwise the disk would be more puffed up than observed. This limit is shown in Figure 3, along with the line that corresponds to having at least one black hole of mass M within the Galaxy.

Although the dependence is not shown explicitly in Equation (6.1), M_heat also scales as σ^2 and ρ_h^{-1}. Thus, by applying the disk-heating argument to galaxies with higher dark matter density, lower stellar velocity dispersion, or smaller age, one can obtain stronger constraints. For the gas-rich dwarf galaxy DD0154 (which has $\sigma = 17 \mathrm{~km~s}^{-1}$, an age of at least 1.5 Gyr, and a central dark matter density of $0.009 M_\odot \mathrm{pc}^{-3}$), Rix & Lake (1993) find $M < 7 \times 10^5 M_\odot$. For the dwarf galaxy GR8 (which has $\sigma = 4 \mathrm{~km~s}^{-1}$, an age of at least 1 Gyr, and a central dark matter density of $0.07 M_\odot \mathrm{pc}^{-3}$), they find $M < 6 \times 10^3 M_\odot$. Of course, unless the black holes form pregalactically, there is no reason for expecting the halo objects to have the same mass in different galaxies, so these limits are not shown in Figure 3.

6.2 *Disruption of Stellar Clusters by Halo Objects*

Another type of dynamical effect associated with halo objects would be their influence on bound groups of stars (in particular, globular clusters and loose clusters). Every time a halo object passes near a star cluster, the object's tidal field heats up the cluster and thereby reduces its binding energy. Over a sufficiently large number of fly-bys this could evaporate the cluster entirely. This process was first discussed by Spitzer (1958) for the case in which the disrupting objects are giant molecular clouds. Carr (1978) used a similar analysis to argue that the halo objects must be smaller than $10^5 M_\odot$ or else loose clusters would not survive as long as observed—but this argument neglected the fact that sufficiently massive holes will disrupt clusters by single rather than multiple fly-bys. The correct analysis was given by Wielen (1985) for halo objects with the mass of $2 \times 10^6 M_\odot$ required in the Lacey-Ostriker scenario and by Sakellariadou (1984) and Carr & Sakellariadou (1994) for halo objects of general mass.

By comparing the expected disruption time for clusters of mass m_c and radius r_c with the typical cluster lifetime t_L, one finds that the local density of halo holes of mass M must satisfy (cf Ostriker et al 1989)

$$\rho_B < \begin{cases} \dfrac{m_c V}{G M t_L r_c} & \text{for} \quad M < m_c \left(\dfrac{V}{V_c}\right) \\ \left(\dfrac{m_c}{G t_L^2 r_c^3}\right)^{1/2} & \text{for} \quad m_c \left(\dfrac{V}{V_c}\right) < M < m_c \left(\dfrac{V}{V_c}\right)^3 \\ \dfrac{m_c^{2/3} M^{1/3}}{(V t_L r_c^2)} & \text{for} \quad M > m_c \left(\dfrac{V}{V_c}\right)^3 . \end{cases} \tag{6.2}$$

Here $V_c \sim (G m_c / r_c)^{1/2}$ is the velocity dispersion within the cluster, V is the speed of the halo objects ($\sim$300 km s^{-1}) and we have neglected numerical factors of order unity. The increasing mass regimes correspond to disruption by multiple encounters, single encounters, and nonimpulsive encounters, respectively. Any lower limit on t_L therefore places an upper limit on ρ_B. The crucial point is that the limit is independent of M in the single-encounter regime, so that the limit bottoms out at a density of order $(\rho_c / G t_L^2)^{1/2}$. The constraint is therefore uninteresting if this exceeds the observed halo density ρ_h. In particular, if the clusters survive for the lifetime of the Galaxy, which is essentially the age of the Universe t_o, the limiting density is just $(\rho_c \rho_o)^{1/2}$, where ρ_o is the mean cosmological density. If t_L is much larger, than t_o, the fraction of clusters disrupted within t_o is $f_c \sim t_o / t_L$ and so the limiting density is reduced by the factor f_c.

The strongest limit is associated with globular clusters, for which we take $m_c = 10^5 M_\odot$, $r_c = 10$ pc, $V_c = 10$ km s^{-1}, and $t_L > 10^{10}$y. We also assume that the holes have a speed $V = 300$ km s^{-1}. Rather remarkably, due to the "coincidence" that the halo density is the geometric mean of the cosmological density and the globular cluster density, the upper limit on ρ_B is comparable to the actual halo density; this suggests that halo objects might actually *determine* the characteristics of surviving globular clusters (cf Fall & Rees 1977). Numerical calculations for the disruption of globular clusters by Moore (1993) confirm the general qualitative features indicated above: gradual mass loss for small halo objects and sudden disruption for larger ones. However, using data for nine particular globular clusters, Moore infers an upper limit of $10^3 M_\odot$. This is in the multiple-encounter regime and considerably stronger than the limit implied by Equation (6.2) with $t_L = t_o$, presumably because his clusters are very diffuse. Because of the uncertainties, the line corresponding to Moore's result is only shown dotted in Figure 3.

6.3 *Effect of Dynamical Friction on Halo Objects*

Another important dynamical effect is that halo objects will tend to lose energy to lighter objects and consequently drift toward the Galactic nucleus (Chandrasekhar 1964). In particular, one can show that halo objects will be dragged into the nucleus by the dynamical friction of the Spheroid stars from within a Galactocentric radius

$$R_{df} = \left(\frac{M}{10^6 M_\odot}\right)^{2/3} \left(\frac{t_g}{10^{10}\mathrm{y}}\right)^{2/3} \mathrm{kpc}, \tag{6.3}$$

and the total mass dragged into the Galactic nucleus is therefore

$$M_N = 9 \times 10^8 \left(\frac{M}{10^6 M_\odot}\right)^2 \left(\frac{t_g}{10^{10}\mathrm{y}}\right)^2 \left(\frac{a}{2\ \mathrm{kpc}}\right)^{-2} M_\odot, \tag{6.4}$$

where a is the halo core radius (Carr & Lacey 1987). This exceeds the upper observational limit of $3 \times 10^6 M_\odot$ (Sellgren et al 1990, Spaenhauer et al 1992) unless

$$\Omega_B < \Omega_h \left(\frac{M}{3 \times 10^3 M_\odot}\right)^{-1} \left(\frac{a}{2\ \mathrm{kpc}}\right) \left(\frac{t_g}{10^{10}\mathrm{y}}\right)^{-1} \tag{6.5}$$

This is certainly stronger than the disk-heating limit; it may also be stronger than the cluster disruption limit.

Although this argument would seem to preclude the Lacey-Ostriker proposal, there is an important caveat in this conclusion (Hut & Rees 1992). Equation (6.4) implies that about 10^3 holes of $10^6 M_\odot$ would have drifted into the Galactic nucleus by now, corresponding to one arrival every 10^7y. Once two black holes have reached the nucleus, they will form a binary, which will eventually coalesce due to loss of energy through gravitational radiation. If a third hole arrives before coalescence occurs, then the "slingshot" mechanism could eject one of the holes and the remaining pair might also escape due to the recoil (Saslaw et al 1974). Hut & Rees estimate that the time for binary coalescence is shorter than the interval between infalls, which suggests that the slingshot is ineffective. However, there is another problem with Equation (6.5): Dynamical friction will also deplete the number of stars in the nucleus and this will eventually suppress dynamical friction unless there is an efficient mechanism to replenish the loss-cone (Begelman et al 1980). Limit (6.5) is clearly not completely firm, so it is only shown dotted in Figure 3.

6.4 *Is the Halo made of Dark Clusters?*

We have seen that both the cluster disruption and dynamical friction constraints may be incompatible with the Lacey & Ostriker proposal that $2 \times 10^6 M_\odot$ halo black holes generate the observed disk-heating. There is also the problem that supermassive halo black holes might generate too much radiation through accretion as they traverse the disk (Ipser & Price 1977). To circumvent these objections, Carr & Lacey (1987) have proposed that the disk heaters are $2 \times 10^6 M_\odot$ *clusters* of smaller objects rather than single black holes. The accretion luminosity is then reduced by a factor of order the number of objects per cluster and the dynamical friction problem is avoided, provided the clusters are disrupted by collisions before they are dragged into the Galactic nucleus by dynamical friction.

One can extend this idea to a more general cluster scenario (Wasserman & Salpeter 1993, Kerins & Carr 1994, Moore & Silk 1994). If we assume that the clusters all have the same mass M_c and radius R_c, then they will be disrupted by collisions within the Galactocentric radius (6.3) at which dynamical friction operates, providing

$$R_c > 1.4 \left(\frac{a}{2\ \text{kpc}}\right)^2 \left(\frac{t_g}{10^{10}\text{y}}\right)^{-1} \text{pc}. \tag{6.6}$$

If this condition is not satisfied, then M_c must be less than the value indicated by Equation (6.5). In order to avoid the evaporation of clusters as a result of 2-body relaxation, one also requires

$$R_c > 0.04 \left(\frac{m}{0.01 M_\odot}\right)^{2/3} \left(\frac{t_g}{10^{10}\text{y}}\right)^{2/3} \left(\frac{M_c}{10^6 M_\odot}\right)^{-1/3} \text{pc}, \tag{6.7}$$

where m is the mass of the components. An *upper* limit on R_c comes from requiring that the clusters do not disrupt at our own Galactocentric radius $R_o \sim 10$ kpc which implies

$$R_c < 35 \left(\frac{R_o}{10\ \text{kpc}}\right)^2 \left(\frac{t_g}{10^{10}\text{y}}\right)^{-1} \text{pc}. \tag{6.8}$$

These dynamical limits, together with the disk-heating limit (6.1), are indicated by the bold lines in Figure 4, which show that the values of M_c and R_c are constrained to a rather narrow range. The cluster-disruption upper limit on M_c is not shown because it is rather model-dependent but it could further reduce the range.

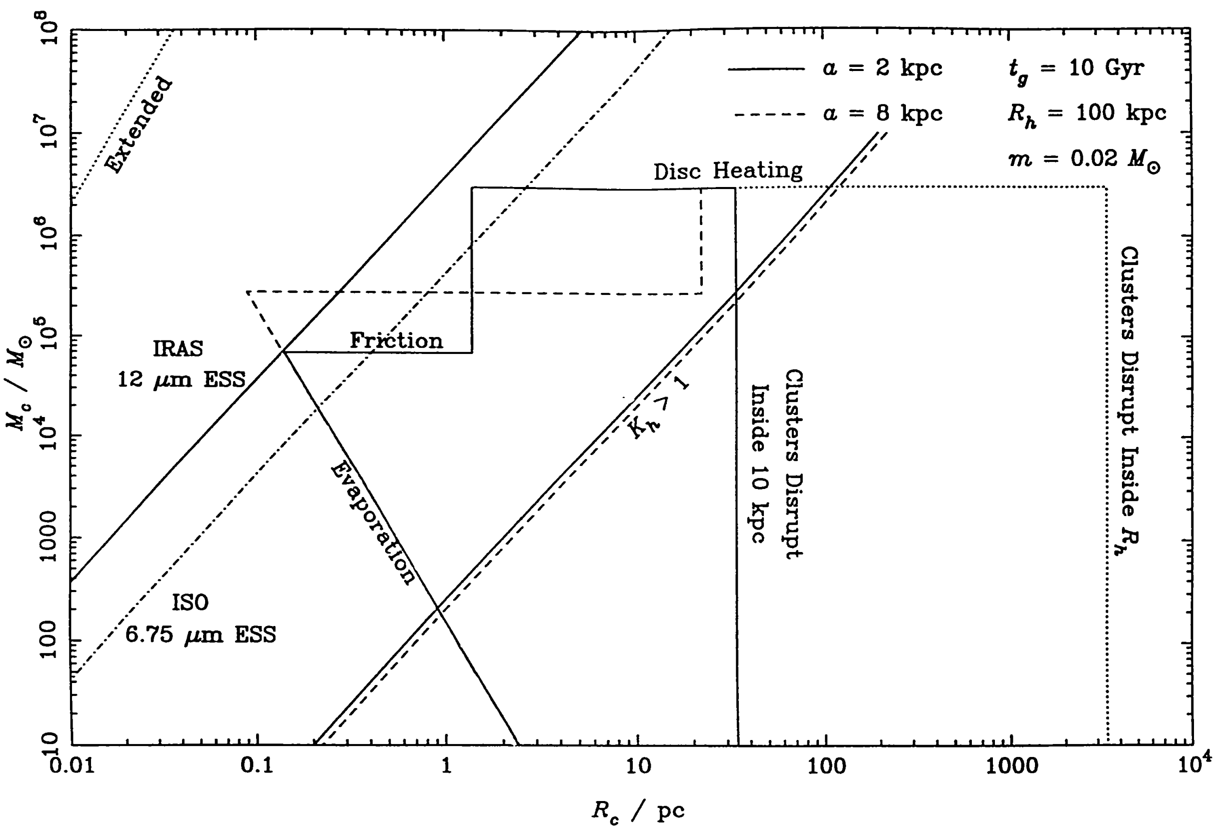

Figure 4 Dynamical constraints on the mass M_c and radius R_c of clusters that provide the dark mass in the Galactic halo. Outside the bold lines the clusters are either disrupted by collisions or produce excessive disk heating or evaporate or produce an excessive buildup of mass in the Galactic nucleus as a result of dynamical friction. Also shown are the extended source sensitivity of *ISO* (for an integration time of 100 s) and *IRAS*, assuming that the brown dwarfs have the optimal mass of $0.02M_{\odot}$, and the region where the clusters cover the sky.

There is some uncertainty in the positions of the boundaries in Figure 4. If one merely requires that the clusters do not disrupt at the edge of the halo, the upper limit (6.8) is increased by a factor of $(R_h/R_o)^2$, as indicated by the dotted line in Figure 4. The dynamical friction limits are sensitive to the value of a: the limits are shown for $a = 2$ kpc and $a = 8$ kpc since this spans the range of likely values. The evaporation limit given by Equation (6.7) depends on the value of m: Figure 4 assumes $m = 0.02M_{\odot}$. Note that together Equations (6.1), (6.7), and (6.8) require the cluster components to be smaller than $10M_{\odot}^2$, which probably excludes their being VMO black holes.

6.5 *Constraints on Dark Objects Outside Halos*

Dynamical constraints on dark objects in the Galactic disk are generally stronger than the halo limits. In particular, Bahcall et al (1985) have argued that the disk dark matter could not comprise objects larger than $2M_\odot$ or else they would disrupt the wide binaries observed by Latham et al (1984). [This limit can be deduced from Equation (6.2) by identifying m_c and r_c with the total mass and separation of the binary.] This is an important constraint because, if correct, it rules out disk dark matter comprising stellar black holes. However, the Bahcall et al conclusion has been disputed by Wasserman & Weinberg (1987) on the grounds that there is no sharp cut-off in the distribution of binary separations above 0.1 pc. The limit is therefore weakened (somewhat arbitrarily) to $10M_\odot$ in Figure 3.

Dynamical constraints on dark objects in clusters of galaxies are weaker than the halo limits. For example, one does not get an interesting constraint by applying Equation (6.2) to the disruption of cluster galaxies by cluster black holes because the upper limit on ρ_B exceeds the cluster density. However, one does get an interesting constraint from upper limits on the fraction of galaxies f_g with unexplained tidal distortions. Equation (6.2) can also be applied in this case, except that the limits are weakened by a factor λf_g^{-1}, where the parameter $\lambda(\sim 2)$ represents the difference between distortion and disruption. Van den Bergh (1969) applied this argument to the Virgo cluster and inferred that black holes binding the cluster could not be bigger than $10^9 M_\odot$. If we assume that Virgo is typical, we obtain the limit indicated in Figure 3. We also show the limit corresponding to the requirement that there be at least one black hole of mass M within the cluster.

The dynamical constraints on intergalactic black holes are even weaker. The most interesting one comes from the fact that, if there were a population of huge intergalactic black holes, each galaxy would have a peculiar velocity due to its gravitational interaction with the nearest one (Carr 1978). If the holes were smoothly distributed and had a number density n, one would expect every galaxy to have a peculiar velocity of order $GMn^{2/3}t_g$. Since the CMB dipole anisotropy shows that the peculiar velocity of our own Galaxy is only 600 km s^{-1}, one infers a limit $\Omega_B < (M/10^{16}M_\odot)^{-1/2}$ and this is also shown in Figure 3. The limit on the bottom right corresponds to the requirement that there be at least one object of mass M within the current particle horizon.

7. GRAVITATIONAL LENSING EFFECTS

One of the most useful signatures of baryonic dark matter candidates is undoubtedly their gravitational lensing effects. Indeed, it is remarkable that lensing could permit their detection over the entire mass range of $10^{-7}M_\odot$ to $10^{12}M_\odot$. All sorts of astronomical objects can serve as lenses (Blandford & Narayan 1992) but the crucial advantage of Population III objects is that they are compact and spherically symmetric, which makes their effects very clean. To search for them, one requires sources that are numerous, small, bright, and have predictable intrinsic variations (Nemiroff 1991a). The most useful sources to date have been quasars, galaxies, radio jets, gamma-ray bursts, and stars; all of these are discussed below. Other possibilities include radio sources (Blandford & Jarosynski 1981), supernovae (Schneider & Wagoner 1987, Linder et al 1988, Rauch 1991), and pulsars (Krauss & Small 1991). There are two distinct lensing effects and these probe different but nearly overlapping mass ranges: *macrolensing* (the multiple-imaging of a source) can be used to search for objects larger than $10^4 M_\odot$, while *microlensing* (modifications to the intensity of a source) can be used for objects smaller than this. The current constraints on the density Ω_c of compact objects in various mass ranges are brought together in Figure 5.

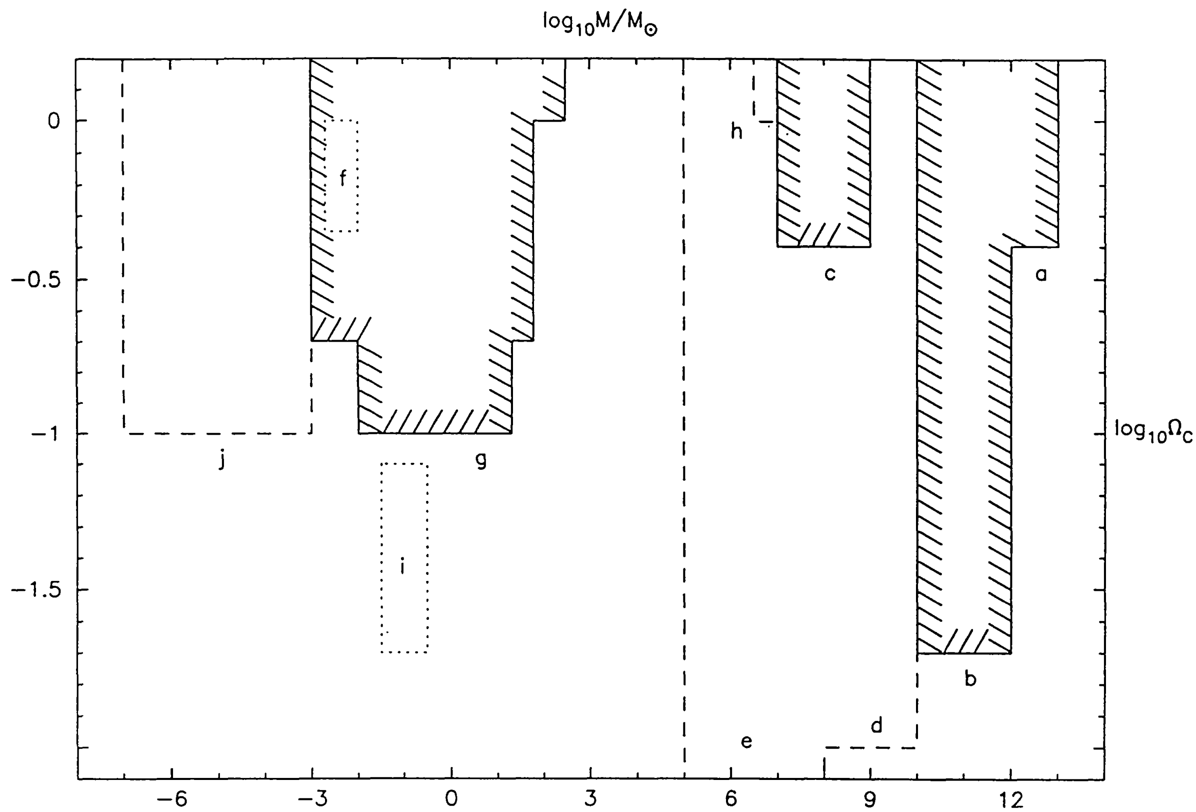

Figure 5 Macrolensing and microlensing constraints on the density parameter for compact objects of mass M. Current limits are shown by shaded lines and potential ones by broken lines. (*a*) VLA limit of Hewitt (1986); (*b*) optical and *HST* limit of Surdej et al (1993); (*c*) VLBI limit of Kassiola et al (1991); (*d*) and (*e*) potential speckle interferometry and VLBA limits; (*f*) region required to explain the quasar variations claimed by Hawkins (1993); (*g*) Dalcanton et al (1994) quasar line-continuum limit; (*h*) gamma-ray burst limit of Nemiroff et al (1993), assuming these are at a cosmolgical redshift; (*i*) corresponds roughly to the range of values required to explain the MACHO and EROS microlensing results; (*j*) potential limit associated with the null results from the EROS CCD study.

7.1 *Macrolensing Constraints on Compact Objects*

If one has a population of compact objects with mass M and density parameter Ω_c, then the probability P of one of them image-doubling a source at redshift $z \approx 1$ and the separation between the images θ are given by

$$P \approx (0.1\text{–}0.2)\Omega_c, \qquad \theta \approx 6 \times 10^{-6} \left(\frac{M}{M_\odot}\right)^{1/2} h^{1/2} \text{ arcsec} \tag{7.1}$$

(Press & Gunn 1973). One can therefore use upper limits on the frequency of macrolensing for different image separations to constrain Ω_c as a function of M. Although optical searches, VLA, and the *Hubble Space Telescope* (*HST*) can only constrain objects down to $10^{10} M_\odot$ (corresponding to a resolution of 0.1 arcsec), speckle cameras (with a resolution of 10^{-2} arcsec) can get down to $10^8 M_\odot$, while VLBI and VLBA (with resolutions of 1 and 0.1 milliarcsec) can search for objects as small as $10^6 M_\odot$ and $10^4 M_\odot$. The best strategy is to look for dim images near bright objects (Nemiroff & Bistolas 1990), which requires a large dynamic range, but one can also look for circular distortions and gravity rings (Saslaw et al 1985, Turner et al 1990). The usual approach is to derive the "detection volume," defined as the volume between the source and observer within which the lens would need to lie in order to produce an observable effect (Nemiroff 1989, Kassiola et al 1991). Limits are then obtained by adding the detection volume for each source and comparing this to the volume per source expected for a given Ω_C.

There have been several optical and radio surveys to search for multiply-imaged quasars (Hewitt et al 1989, Bahcall et al 1992b). In particular, Hewitt (1986) used VLA observations to infer $\Omega_C(10^{11}\text{–}10^{13} M_\odot) < 0.4$, Nemiroff (1991b) used optical QSO data from Crampton et al (1989) to infer $\Omega_C(M > 10^{9.9} M_\odot) < 1$ and $\Omega_C(M > 10^{10.3} M_\odot) < 0.25$, and Surdej et al (1993) used data on 469 highly luminous quasars (including *HST* observations) to infer $\Omega_C(10^{10}\text{–}10^{12} M_\odot) < 0.02$. To probe smaller scales, one must use high resolution radio sources: Kassiola et al (1991) have used lack of lensing in 40 VLBI objects to infer $\Omega_C(10^7\text{–}10^9 M_\odot) < 0.4$, while a study by Patnaik et al (1992) of 200 flat spectrum radio sources may lead to a limit $\Omega_C(10^6\text{–}10^9 M_\odot) < 0.01$ (Henstock et al 1993). (Flat spectrum sources are dominated by a single core and are therefore more likely to be lensed; this limit assumes that no sources are identified and is not included in Figure 5.)

Future observations could strengthen these constraints considerably: Speckle interferometry could push $\Omega_C(10^8\text{–}10^{10} M_\odot)$ down to 0.01, while VLBA could push $\Omega_C(10^5\text{–}10^8 M_\odot)$ down to 0.001 (Surdej et al 1993). These two limits are shown as broken lines in Figure 5. Another interesting possibility is to search for lensing distortions in radio jets (Kronberg et al 1991); this would permit the detection of objects with mass around $10^6 M_\odot$ since the Einstein radius for such objects is of order milliarcsecs and therefore comparable to the characteristic jet scale. Of course, jets may be intrinsically kinky but Wambsganss & Paczynski (1992) have pointed out that this poses no problem if one uses VLBI and VLBA maps of the jets in image-doubled quasars because only one of the images would then be kinked. Their numerical simulations show that the effects of supermassive black holes would be numerous and obvious. Lenses between 0.3 and $3 \times 10^6 M_\odot$ would certainly be noticeable for a dynamic range of 100:1 and may have already been excluded (Heflin et al 1991, Garrett et al 1994).

7.2 *Microlensing in Macrolensed Quasars*

Even if a lens is too small to produce resolvable multiple images of a source, it may still induce detectable intensity variations. In particular, one can look for microlensing in quasars that are already macrolensed. This possibility arises because, if a galaxy is suitably positioned to image-double a quasar, then there is also a high probability that an individual halo object will traverse the line of sight of one of the images (Gott 1981); this will give intensity fluctuations in one but not both images. Although the effect would be observable for objects bigger than $10^{-4} M_\odot$, the timescale of the fluctuations is around $40(M/M_\odot)^{1/2}$y, and this would exceed a decade for $M < 0.1 M_\odot$.

There is already evidence of this effect for the quasar 2237+0305 (Irwin et al 1989). This has four images at a redshift of 1.7 and the lens is a galaxy at redshift 0.04. The brightest image brightened by 0.5 magnitudes from September, 1987 to August, 1988 and then dimmed by 0.15 magnitudes by September, 1988. There was no variation in the other images, even though the difference in light-travel time is only hours. The observed timescale for the variation indicates a mass in the range $0.001 M_\odot$ to $0.1 M_\odot$, although Wambsganss et al (1990) argue that it might be as high as $0.5 M_\odot$, the mass where a standard IMF gives the dominant contribution. (The variable image is almost exactly aligned with the center of the lensing galaxy, where the density should be dominated by ordinary stars). Analysis of more extensive data (Corrigan et al 1991) has strengthened the evidence for microlensing with a mass below $0.1 M_\odot$ (Webster et al 1991).

7.3 *The Effect of Microlensing on Quasar Luminosity*

Evidence for the microlensing of unmacrolensed quasars may come from studying their luminosity variations (Peacock 1986, Kayser et al 1986, Schneider & Weiss 1987, Refsdal & Starbell 1991, Lewis et al 1993), and there may already be cases of this. In particular, Nottale (1986) claims that lensing by low mass objects may explain some optically violently variable quasars. For example, the quasar 0846+51 brightened by 4 magnitudes in a month and then dimmed by 1 magnitude in a few days. The fact that its line of sight is only 12 arcsec from a galaxy suggests that the variation may result from microlensing by one of the halo objects, in which case the mass of the halo object must be in the range 10^{-4} to $10^{-2} M_{\odot}$.

More dramatic, but no less controversial, evidence for the effect of microlensing on quasar luminosity comes from Hawkins (1993), who has been monitoring 300 quasars in the redshift range 1–3 over the past 17 years using a wide-field Schmidt camera. He finds quasi-sinusoidal variations of amplitude 0.5 m on a 5y timescale and he attributes this to lenses with mass $\sim 10^{-3} M_{\odot}$. The crucial point is that the timescale decreases with increasing z, which is the opposite to what one would expect for intrinsic variations (and these would be on a shorter timescale anyway). The timescale also increases with the luminosity of the quasar. He tries to explain this by noting that the luminosity should increase with the size of the accretion disk, but this only works if the disk is larger than the Einstein radius of the lens (about 0.01 pc), which is questionable. Another worrisome feature of Hawkins' claim (cf Schneider 1993) is that he requires the density of the lenses to be close to critical (so that the sources are being transited continuously). In this case, Big Bang nucleosynthesis constraints require the lenses to be nonbaryonic, so he is forced to invoke primordial black holes.

7.4 *The Effect of Microlensing on Quasar Density*

Quasars that are not bright enough to be included in a flux-limited sample may be amplified by quasar microlensing, thereby bringing them above the detection threshold (Turner 1980, Canizares 1981, Peacock 1982, Schneider et al 1992) and modifying the apparent number density. This effect depends strongly on the quasar luminosity function, which may itself be influenced by lensing (Vietri & Ostriker 1983). There are several indications that this happens. For example, Webster et al (1988) found that faint galaxies were 4.4 times as numerous as usual within 6 arcsec of high redshift quasars and attributed this to the galaxies enhancing the quasar density. However, to explain such a high enhancement, they had to attribute to the galaxies unrealistically massive halos (Hogan et al 1989), so the origin of this effect is not well understood.

A similar result was found by Hammer & Le Fevre (1990), who found the quasar density within 5 arcsec of $z > 1$ radio galaxies to be nine times greater than expected; Bartleman & Schneider (1993) claim that this can be explained if the quasar luminosity function is sufficiently steep. Rix & Hogan (1988) have claimed a *lower* limit of $\Omega_C(0.001–10^{10} M_{\odot}) > 0.25$ from an excess of quasar-galaxy pairs in the Einstein Medium Source Survey, but Dalcanton et al (1994) argue that they underestimate the amplification (and hence overestimate Ω_C) by underestimating the steepness of the quasar luminosity function. Kovner (1991) obtains constraints on $\Omega_C(0.001–10^{10} M_{\odot})$ by studying the slope of the bright quasar counts.

Rodrigues-Williams & Hogan (1994) have found an excess of quasars in the direction of clusters. Their sample comprises 129 quasars with $1.4 < z < 2.2$

and 70 clusters at $z \sim 0.2$; they find an overdensity of 1.7. Unfortunately, this does not seem to be consistent with the most plausible mass distribution. Note that there is also a lensing effect that reduces the number of quasars near clusters because the background area is expanded. Which effect wins depends on the steepness of the quasar luminosity function. The amplification effect wins when the luminosity function is steep, but the spread effect wins when it is shallow. There may also be evidence for the second effect: Boyle et al (1988) have found a 30% deficit of high redshift quasars within 4 arcsec of clusters, although they attribute this to the effect of dust.

7.5 *Line-to-Continuum Effects of Quasars*

In some circumstances, only part of the quasar may be microlensed. In particular, the line and continuum fluxes may be affected differently because they may come from regions that act as extended and pointlike sources, respectively. [For a lens at a cosmological distance, the Einstein radius is $0.05(M/M_\odot)^{1/2}h$ pc, whereas the size of the optical continuum and line regions are of order 10^{-4} pc and 0.1–1 pc, respectively.] This effect can be used to probe individual sources. For example, the variations in the line-to-continuum ratio for different images of the same macrolensed quasar can be used to constrain the mass of the objects in the lensing galaxy. Evidence for such an effect may already exist in the case of the double quasar 2016 + 112, where variations in the intensity ratios for the different images suggest that the lensing objects have a mass in the range $3 \times 10^4 M_\odot$ to $3 \times 10^7 M_\odot$ (Subramanian & Chitre 1987).

The line-continuum effect can also show up in statistical studies of many quasars and there is one particularly important effect in this context. One would expect the characteristic equivalent width of quasar emission lines to decrease as one goes to higher redshift because there would be an increasing probability of having an intervening lens. Indeed, a third of quasars should have equivalent widths smaller by 2–3 at only a moderate redshift if $\Omega_C = 1$. This idea was first studied by Canizares (1982). More recently, Dalcanton et al (1994) have compared the equivalent widths for a high and low redshift sample comprising 835 Einstein Medium Source Survey quasars and 92 Steidel-Sargent absorption systems and find no difference. They infer the following limits:

$$\Omega_C(0.001\text{–}60M_\odot) < 0.2, \quad \Omega_C(60\text{–}300M_\odot) < 1,$$
$$\Omega_C(0.01\text{–}20M_\odot) < 0.1. \tag{7.2}$$

The mass limits come from the fact that the amplification of even the continuum region would be unimportant for $M < 0.001M_\odot$, while the amplification of the broad-line regions would be important (cancelling the effect) for $M > 20M_\odot$ if $\Omega_c = 0.1$, for $M > 60M_\odot$ if $\Omega_c = 0.2$ or for $M > 300M_\odot$ if $\Omega_c = 1$. (These limits are indicated in Figure 5). This compares with the earlier Canizares

(1982) constraint of $\Omega_C(0.01\text{–}10^5 M_\odot) < 1$; his upper mass limit was larger because the size of the broad-line region was thought to be larger then. Note that Equation (7.2) is incompatible with Hawkins' claim that $\Omega_C(10^{-3} M_\odot) \sim 1$, although one would only need to reduce Ω_C or M slightly.

7.6 *Microlensing of Gamma-Ray Bursts*

Another method of seeking evidence for compact objects in the mass range $10^6\text{–}10^8 M_\odot$ is to look for echoes from gamma-ray bursts (on the assumption that these are at cosmological distances). The images can be resolved temporally but not spatially (Paczynski 1987). This effect has been considered by many people (Webster & Fitchett 1986, Krauss & Small 1991, Blaes & Webster 1991, Mao 1992, Gould 1992, Narayan & Wallington 1992). The most recent analysis is that of Nemiroff et al (1993), who find no evidence for echoes in data for 44 bursts discovered by the *Gamma Ray Observatory*. Using the detection volume technique and theoretical redshifts for the bursts, they infer a limit $\Omega_C(10^{6.5}\text{–}10^{8.1} M_\odot) < 1$, which is shown in Figure 5. However, it must be stressed that the redshifts of the bursts are quite uncertain (they may not even be cosmological) and, for any particular burst, all one can strictly infer is a constraint on M as a function of redshift.

7.7 *Microlensing of Stars by Halo Objects in our own Galaxy*

Attempts to detect microlensing by objects in our own halo by looking for intensity variations in stars in the Magellanic Clouds and the Galactic Bulge have now been underway for several years and may already have met with success. In this case, the timescale for the variation is $P = 0.2(M/M_\odot)^{1/2}$y, so one can seek lenses over the mass range $10^{-8}\text{–}10^2 M_\odot$, but the probability of an individual star being lensed is only $\tau \sim 10^{-6}$, so one has to look at many stars for a long time (Paczynski 1986). The likely event rate is $\Gamma \sim N\tau P^{-1} \sim (M/M_\odot)^{-1/2}\text{y}^{-1}$, where $N \sim 10^6$ is the number of stars. Thus, small masses give frequent short-duration events (e.g. $0.01 M_\odot$ events would last a week and occur a few times a year) and are best sought with CCDs, while large masses give rare long-duration events (e.g. $10 M_\odot$ events would last a year and occur every few years) and are best sought with photographic plates. The key feature of these microlensing events is that the light-curves are time-symmetric and achromatic; this may allow them to be distinguished from intrinsic stellar variations (Griest 1991).

Three groups are involved; each now claims to have detected lensing events. The American group (MACHO) has used a dedicated telescope at Mount Stromlo to study 10^7 stars in red and blue light in the LMC, the SMC, and the Galactic Bulge. After analyzing 4 fields near the center of the LMC (2×10^6 stars with 250 observations per star), they have obtained one event (Alcock et al 1993): The duration is 34 days (corresponding to a mass of $0.1M_\odot$) and the amplification is $A = 6.8$. The French group (EROS) has been studying stars in the LMC and their approach is two-pronged: They are seeking 1–100 day events (corresponding to 10^{-4}–$1M_\odot$ lenses) with digitized red and blue Schmidt plates obtained with the ESO telescope in Chile and 1 hour to 3 day events (corresponding to 10^{-7}–$10^{-3}M_\odot$ with CCDs taken at the Observatoire de Haute Provence. The CCD searches have given no results, which presumably implies a limit $\Omega_C(10^{-7}$–$10^{-3}M_\odot) < 0.1$, but analysis of 3×10^6 stars on the Schmidt plates yields two events (Auborg et al 1993): One is associated with a main-sequence star and has $A = 2.5$ and $P = 54$ d (corresponding to a mass of $0.2M_\odot$); the other is associated with a star between the main-sequence and the giant branch and has $A = 3.3$ and $P = 60$ d (corresponding to a mass of $0.3M_\odot$). They have also confirmed the MACHO event in red light. The Polish collaborative (OGLE) are using the Las Companas telescope in Chile to look at 7×10^5 stars in the Galactic bulge (Udalski et al 1993). They have claimed one event with $A = 2.4$ and $P = 42$ d (corresponding to a mass of $0.3M_\odot$) which they attribute to a disk M-dwarf, but they only have data in one color. The rough values of M and Ω_c for these events are indicated in Figure 5, but there is considerable uncertainty in both these values.

8. THE BLACK HOLE SCENARIO

One of the most important signatures of the black hole scenario would be the infrared/submillimeter background generated by the stellar precursors. In Section 5.1 we discussed a general constraint on $\Omega_*(M)$, which depended only on the fact that the background light must appear in *some* waveband. Here we discuss more precise constraints for VMOs, exploiting the fact that we can predict the waveband in this case very exactly. The calculation can be extended to cover the mass range below $100M_\odot$, but that range may be excluded by nucleosynthetic constraints anyway. We also consider the generation of gravitational radiation by VMO or SMO black holes.

8.1 *Background Light Observations*

The detection of cosmological background radiation in the IR and submillimeter bands is difficult because of foregrounds from scattered zodiacal light (ZL), interplanetary dust (IPD), and interstellar dust (ISD). Estimates of these competing backgrounds are shown in Figure 6, where the background light intensity $I(\lambda)$ has been expressed in critical density units by defining a quantity $\Omega_R(\lambda) \equiv 4\pi\lambda I(\lambda)/c^3\rho_{crit}$. One sees that there are minima at around 4μ, 100μ, and 400μ, so these are the best "windows" in which to search for an extragalactic background. Although positive detections have been claimed in all of these windows, none has been subsequently confirmed, so only upper limits on $\Omega_R(\lambda)$

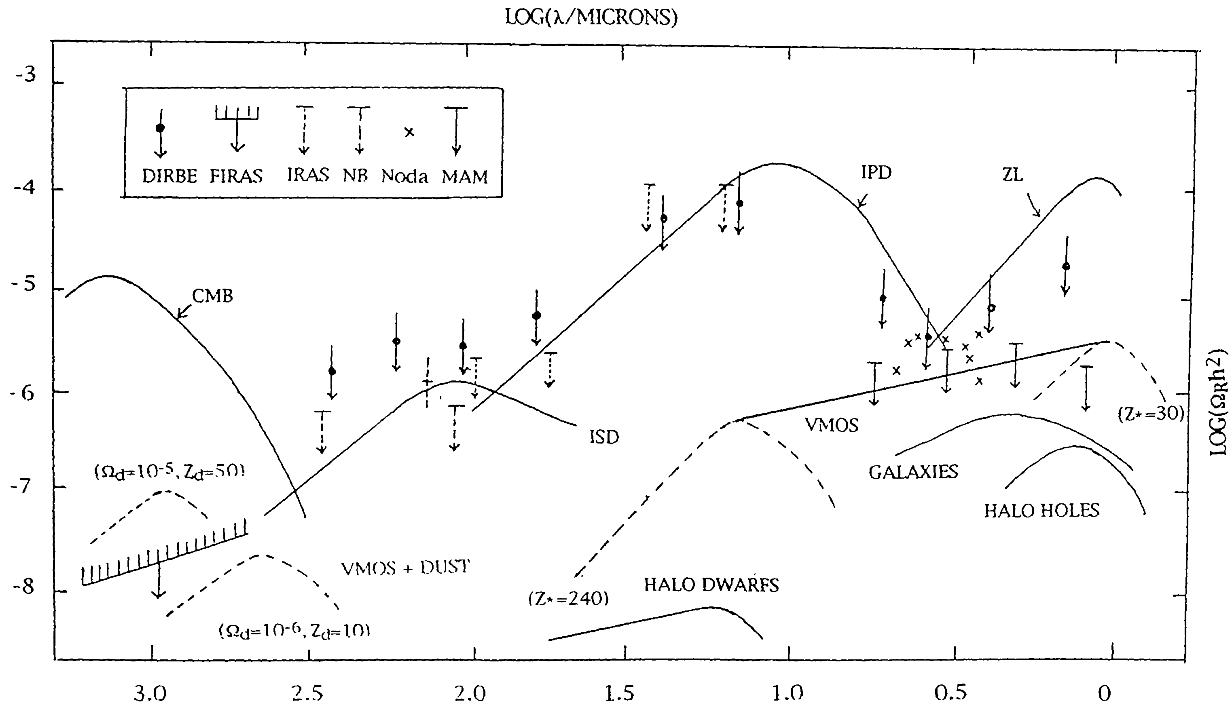

Figure 6 Comparison of the observational constraints on the extragalactic background radiation density from *DIRBE*, *FIRAS*, *IRAS*, Nagoya-Berkeley (NB), Matsumoto et al (MAM), and Noda et al with the background expected in the VMO scenario for different dust abundances. Also shown are the CMB, the local foregrounds, and the background from galaxies, accreting $10^6 M_\odot$ halo black holes, and $0.08 M_\odot$ halo BDs.

are currently available; we begin by summarizing these. For comparison, the CMB peaks at $\lambda_{\text{peak}} = 1400\mu$ with a density $\Omega_R = 2 \times 10^{-5} h^{-2}$.

The *FIRAS* results (Mather et al 1990, 1994) imply that the CMB is so well fit by a black-body spectrum that any extra background must have an intensity less than 0.03% of the CMB density over the range 500–5000μ. This implies $\Omega_R(\lambda) < 6 \times 10^{-9} h^{-2} (\lambda/\lambda_{\text{peak}})^{-1}$. The *DIRBE* results at the south ecliptic pole (Hauser et al 1991) give upper limits in the J, K, L, M, 12μ, 25μ, 60μ, 100μ, 120–200μ and 200–300μ bands. However, the limits indicated in Figure 6 are very conservative since they do not include any subtraction for the foreground backgrounds from interstellar and interplanetry dust. Careful modeling of these foreground contributions may improve the limits. Figure 6 includes the limits derived by Oliver et al (1992) by using *IRAS* and *DIRBE* data in conjunction with detailed dust models. It also shows the limits obtained from an analysis (Lange et al 1991) of the Nagoya-Berkeley rocket data (Matsumoto et al 1988a). At one stage *IRAS* data seemed to indicate a 100μ background with $\Omega_R(100\mu) = 3 \times 10^{-6} h^{-2}$ (Rowan–Robinson 1986) but this is inconsistent with the *DIRBE* results.

The *DIRBE* and *IRAS* limits are very weak around 12μ and 25μ because the interplanetary dust emission is so large. In the near-IR, a Japanese rocket experiment (Matsumoto et al 1988b) gave a limit $\Omega_R(1\text{–}5\mu) < 3 \times 10^{-5}h^{-2}$ with the possible detection of a "line" at 2.2μ with $\Omega_R(2.2\mu) = 3 \times 10^{-6}h^{-2}$. However, this claim was always controversial because of the problem of subtracting starlight and rocket exhaust. Recent observations by Noda et al (1992) give $\Omega_R(1.6\text{–}4.7\mu) < 3 \times 10^{-6}h^{-2}$, which seems to exclude such a line.

8.2 *Infrared Background from VMOs*

We now compare these limits with the background expected from a population of VMOs. This can be predicted very precisely since all VMOs have a surface temperature T_s of about 10^5K and generate radiation with efficiency $\varepsilon \approx 0.004$. We normalize the VMO density parameter to the value $\Omega_* \approx 0.1$ required to explain galactic halos and assume that they produce black-body radiation with temperature T_s. If the radiation is affected only by cosmological redshift, its density and peak wavelength at the present epoch should be

$$\Omega_R(\lambda_{\text{peak}}) = 4 \times 10^{-6} \left(\frac{\Omega_*}{0.1}\right) \left(\frac{1+z_*}{100}\right)^{-1},$$
$$\lambda_{\text{peak}} = 4 \left(\frac{1+z_*}{100}\right) \mu, \tag{8.1}$$

where z_* is the redshift at which the VMOs burn. We can place an *upper* limit on z_* by noting that the main-sequence time of a VMO is $t_{\text{MS}} \approx 2 \times 10^6$y (independent of mass), so that z_* cannot exceed the redshift when the age of the Universe is t_{MS}. This implies $z_* < 240h^{-2/3}$ and so $\lambda_{\text{peak}} < 15\mu$ and $\Omega_R > 10^{-6}$ for $h > 0.5$. We can place a lower limit on z_* from UV/optical background light limits. As discussed by McDowell (1986) and Negroponte (1986), these imply a constraint on the density of VMOs burning at any redshift z_*. If one requires $\Omega_* \approx 0.1$, this places a lower limit on z_*, mainly because one needs the radiation to be redshifted into the near-IR band, where the background light limits are weaker. In the absence of neutral hydrogen absorption, one requires $z_* > 30$, which implies $\lambda_{\text{peak}} > 1\mu$ and $\Omega_R < 10^{-5}$. The peak of the VMO background must then lie somewhere on the heavy line in Figure 6 and the spectrum must lie within the region bounded by the broken line. Note that the observational limits are only just beginning to constrain the VMO scenario and they may never be able to exclude it if z_* is so large (>200) that most of the VMO light is pushed beyond 10μ, where it would be hidden by interstellar dust.

The constraints on the VMO scenario would be much stronger if the light was reprocessed by dust as discussed by many workers (McDowell 1986, Negroponte 1986, Bond et al 1986 Wright & Malkan 1987, Lacey & Field 1988, Adams et al 1989, Draine & Shapiro 1989). Such dust could either be pregalactic in origin or confined to galaxies themselves if galaxies cover the sky. If the dust cross-section for photons of wavelength λ is assumed to be geometric (πr_d^2 for a grain radius $r_{\rm d}$) for $\lambda \gg r_{\rm d}$, but to fall off as λ^{-1} for $\lambda \gg r_{\rm d}$ then the spectrum should peak at a present wavelength (Bond et al 1986)

$$\lambda_{\rm peak} = 400 \left(\frac{1+z_*}{100}\right)^{1/5} \left(\frac{r_{\rm d}}{0.01\mu}\right)^{1/5} \left(\frac{1+z_{\rm d}}{10}\right)^{1/5} \mu, \tag{8.2}$$

where $z_{\rm d}$ is the epoch of dust production and we have used Equation (8.1) with $\Omega_* \approx 0.1$ to express $\Omega_{\rm R}$ in terms of z_*. The crucial point is that the wavelength is very insensitive to the various parameters appearing in Equation (8.2) because the exponents are so small. At one time the Nagoya-Berkeley experiment (Matsumoto et al 1988a) appeared to indicate a submillimeter excess peaking at almost exactly the wavelength predicted. However, the Nagoya-Berkeley excess has now been disproved by *FIRAS* and the question arises of whether the VMO-plus-dust scenario is still compatible with *COBE* results.

It should be stressed that one does not necessarily expect dust reprocessing anyway. Pregalactic dust with density $\Omega_{\rm d}$ would only absorb UV photons for

$$z_{\rm d} > 10 \left(\frac{\Omega_{\rm d}}{10^{-5}}\right)^{-2/3} \left(\frac{r_{\rm d}}{0.1\mu}\right)^{2/3}, \tag{8.3}$$

where $\Omega_{\rm d}$ is normalized to the sort of value appropriate for galaxies. It is not clear whether this condition can be satisfied. One has no direct evidence for pregalactic dust but in any hierarchical clustering picture one would expect at least some pregalactic dust production (Najita et al 1990). For example, one could envisage the dust produced by the first dwarf galaxies being blown into intergalactic space because the gravitational potential of the dwarfs would be so small. The dust in galaxies themselves would suffice to reprocess the VMO background only if galaxies cover the sky which—for galaxies like our own—requires the redshift of galaxy formation to exceed about 10 (Ostriker & Heisler 1984, Heisler & Ostriker 1988, Ostriker et al 1990). Even if galaxies do cover the sky, the analysis of Fall et al (1989) indicates that the dust-to-gas ratio in primordial galaxies may only be 5–20% that of the Milky Way for $2 < z < 3$, which makes the opaqueness condition difficult to satisfy.

In general, one would expect there to be both a far-IR dust background and a near-IR attenuated starlight background, with the relative intensity reflecting the efficiency of dust reprocessing. By changing the amount of dust, one can redistribute the light between the near-IR and far-IR in an attempt to obviate the constraints. In order to examine the issue in more detail, Bond et al (1991) have carried out a more sophisticated analysis, in which the dust cross section is assumed to scale as $\lambda^{-\alpha}$ at infrared wavelengths. They also introduce a more realistic model for the source luminosity history, allowing for both "burst" and "continuous" models. Comparison with the far-IR and *COBE* constraints is shown in Figure 6 for two of their models with $\alpha = 1.5$ and $z_* = 100$. One has $\Omega_d = 10^{-5}$ and $z_d = 50$ (which is above the *FIRAS* constraint); the other has $\Omega_d = 10^{-6}$ and $z_d = 10$ (which is below it). This shows that the VMO-plus-dust scenario is only viable for models with a high redshift of energy release ($z_* = 100$) and small amounts of dust ($\Omega_d = 10^{-6}$). Of the models considered by Bond et al (1991), Wright et al (1994) claim that only their model 12 still survives.

8.3 *Generation of 3K Background*

If the dust-reprocessed radiation is itself absorbed by the dust, then the radiation could be completely thermalized, leaving no residual distortions at all. Some people have therefore proposed that the *entire* CMB is grain-thermalized starlight (Layzer & Hively 1973, Rees 1978). This is possible in principle—and Equation (8.1) shows that this idea is certainly not precluded energetically—but the grains would have to form at a high redshift and be very elongated in order to thermalize at long wavelengths (Wright 1982, Hoyle & Wickramsinghe 1989 Hawkins & Wright 1988, Arp et al 1990). The *FIRAS* results now make this model rather hard to sustain. An alternative proposal is that black hole accretion generates the CMB at a somewhat higher redshift ($z \sim 10^3$), when thermalization by free-free processes is possible (Carr 1981b). Of course, any scheme that envisages the CMB deriving from Population III stars or black holes also requires that the early Universe be cold or tepid (with the primordial photon-to-baryon ratio being much less than its present value of 10^9). In this case, one must also invoke VMOs or their remnants to generate the observed light element abundance, as discussed in Section 5.2.

8.4 *Gravitational Radiation from Black Holes*

The formation of a population of black holes of mass M at redshift z_B would be expected to generate bursts of gravitational radiation with a characteristic period and duration:

$$P_o \approx 10GM\frac{(1+z_B)}{c^3} \approx 10^{-2}\left(\frac{M}{10^2 M_\odot}\right)(1+z_B)\text{ s.} \tag{8.4}$$

One can show that the expected time between bursts (as seen today) is less than their characteristic duration provided that $\Omega_B > 10^{-2}\Omega^{-2}$, where Ω is the total density parameter. (Bertotti & Carr 1980). If the holes make up galactic halos, one would therefore expect the burst to form a background of waves with present density $\Omega_g = \varepsilon_g \Omega_B (1+z_B)^{-1}$, where ε_g is the efficiency with which the collapsing matter generates gravity waves. If ε_g were as high as 0.1, the background could be detectable by ground-based laser interfreometers (e.g. LIGO) for M below $10^3 M_\odot$, by Doppler tracking of interplanetary spacecraft (e.g. *Cassini*) for M in the range 10^5–$10^{10} M_\odot$, and by pulsar timing for M

above $10^9 M_\odot$. The observable domains are indicated in Figure 7 and the dotted lines indicate how the predicated backgrounds depend on M and z_B. Note that the value of ε_g is very uncertain and it is probably well below 0.1 for isolated collapse.

The prospects of detecting the gravitational radiation would be much better if the holes formed in binaries (Bond & Carr 1984). This is because two sorts of radiation would then be generated: (*a*) continuous waves as the binaries spiral inward due to quadrupole emission; and (*b*) a final burst of waves when the components finally merge. The burst would have the same characteristics as that associated with isolated holes but it would be postponed to a lower redshift and ε_g would be larger (~ 0.08) because of the larger asymmetry; both factors would increase Ω_g. The continuous waves would also be interesting since they would extend the spectrum to longer periods, thus making the waves detectable by a wider variety of techniques. Over most wavebands, the spectrum of the waves would be dominated by binaries whose initial separation is such that they are coalescing at the present epoch. This corresponds to a separation $a_{crit} = 10^2 (M/10^2 M_\odot)^{3/4} R_\odot$. The total background generated by the binaries

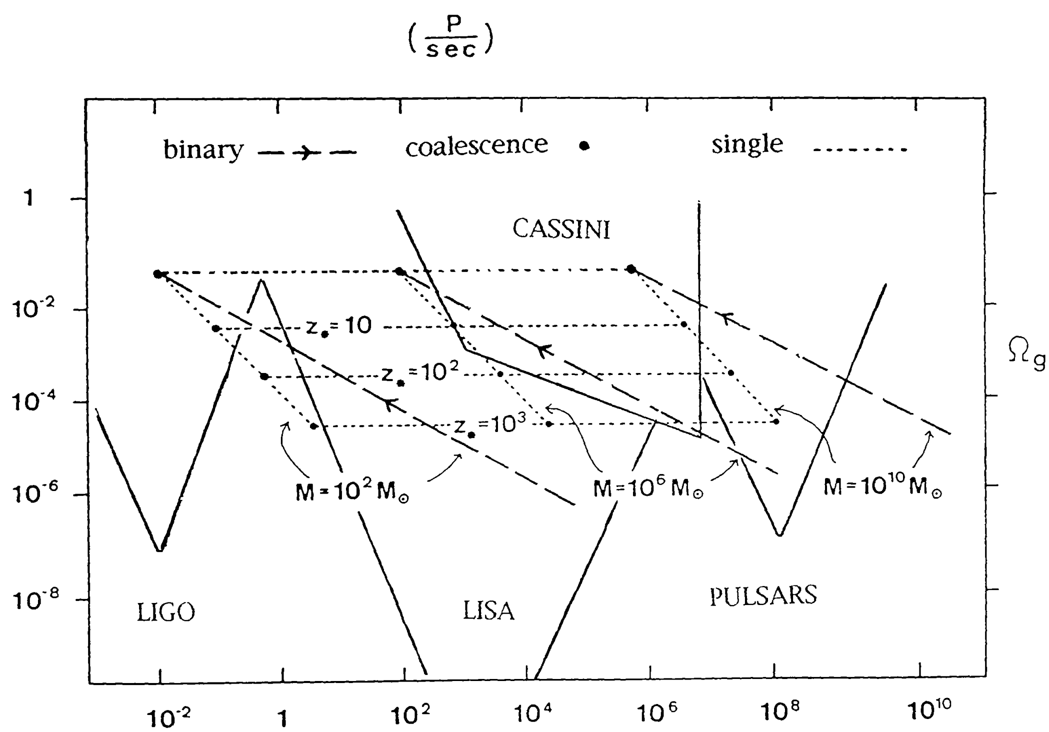

Figure 7 The spectrum of background gravitational waves generated by isolated black holes and coalescing binary black holes. In the first case, we assume that the holes have $\Omega_B = 1$ and that they form at a redshift z_*. In the second case, we assume that the binaries have the separation a_{crit} such that they coalesce at the present epoch. Also shown are the (Ω_g, P) domain accessible to ground-based interometry, Doppler tracking of interplanetary spacecraft, pulsar timing, and space-based interferometry.

is also shown in Figure 7: For each value of M, $\Omega_g(P)$ goes as $P^{-2/3}$, as indicated by the broken lines. Providing the fraction of binaries f_{crit} with around the critical separation is not too small, the background should be detectable by LIGO for $M < 10^3 M_\odot$, by *Cassini* for $10^5 M_\odot < M < 10^{10} M_\odot$, by LISA for $M_\odot < M < 10^{10} M_\odot$, and by pulsar timing for $M > 10^6 M_\odot$.

One could also hope to observe coalescences occurring at the present epoch. For our own halo, the average time t_{burst} between bursts and their expected amplitude h_{burst} would be

$$t_{burst} = 10 \left(\frac{M}{10^2 M_\odot} \right) f_{crit}^{-1} h^{-1} \mathrm{y}, \quad h_{burst} = 7 \times 10^{-17} \left(\frac{M}{10^2 M_\odot} \right). \tag{8.5}$$

Although the time would be uncomfortably long, one could also detect bursts from the Virgo cluster every $4(M/10^2 M_\odot)$ days with somewhat improved sensitivity. Haehnelt (1994) has argued that LISA could detect coalescence bursts throughout the Universe for M in the range 10^3–$10^6 M_\odot$.

9. LOW MASS OBJECTS

In this section, we focus specifically on the Low Mass Object (LMO) scenario. There are several reasons why LMOs currently seem to be the most plausible option. Firstly, there may be direct evidence from cluster cooling flows that baryons can turn into low mass stars with high efficiency even at the present epoch. [This topic is reviewed by Fabian (1994) in this volume, so I merely summarize the key points below and omit references.] Secondly, recent data on the stellar IMF in our own Galaxy suggests there may be a higher fraction of LMOs when the metallicity is low. Thirdly, as we saw in Section 7, microlensing data may already indicate that there is dark matter in the form of LMOs.

9.1 *Cooling Flows in Clusters*

X-ray observations suggest that the cores of many clusters contain hot gas which is flowing inwards because the cooling time is less than the Hubble time. This condition is satisfied in 70–80% of *EXOSAT* clusters and in some poor clusters and groups as well. Direct evidence for cooling comes from Fe XVII line emission, since this shows that the temperature decreases as one goes inwards. The mass flow rates are typically in the range 50–100 $M_\odot y^{-1}$, extending up to $10^3 M_\odot y^{-1}$ in some cases, and they seem to have persisted for at least several billion years. There is consistency between the flow rates derived from spectral measurements and those derived from surface brightness analysis.

The mass appears to be deposited over a wide range of radii with a roughly $M \propto R$ distribution (which requires that the gas be very inhomogeneous), but it cannot be going into stars with the same mass spectrum as in the solar neighborhood, or else the central regions would be bluer and brighter than observed. Some cooling flows do exhibit a blue optical continuum over the central few kpc, but the associated massive star formation rate must be less than a few $M_\odot y^{-1}$, which is only a fraction of the total inflow rate. This suggests that the cooling flows produce very low mass stars, possibly because the high pressure (of order $10^6 \mathrm{cm}^{-3}$K) reduces the Jeans mass. An important feature of a cooling flow is that it is quasi-static, in the sense that the cooling time exceeds the local dynamical time, and it is this condition which is supposed to preserve the high pressure. The Jeans mass could be as low as $0.1 M_\odot$ if the cloud gets as cool as the microwave background radiation ($T = 3$ K); this is not inconceivable because observations suggest that the gas is mainly molecular, which could allow grains to form abundantly.

A recent twist in this scenario has been the detection of large amounts of cold X-ray absorbing material in many clusters (White et al 1991). The cold gas extends out to 100 kpc and the mass involved is usually around $10^{12} M_\odot$ (comparable to that expected from a cooling flow that has persisted for a cosmological time). This raises the question of whether we still need low mass stars, especially in view of the Pfenniger et al (1994) proposal that the dark matter in galactic halos could be cold gas. Of course, if cooling flows do make low mass stars, one might expect some cold gas as an intermediate state. This issue has yet to be resolved.

9.2 *Pregalactic and Protogalactic Cooling Flows*

Although cooling flows provide a natural way of turning gas into low mass stars with high efficiency, those observed in the centers of clusters could not themselves be responsible for either the cluster dark matter (since this is distributed throughout the cluster) or the halo dark matter in galaxies outside clusters. In order to account for the usual dark matter problems, one therefore needs cooling flows on the scale of galaxies or below. Only the most massive cluster galaxies exhibit cooling flows at the present epoch—but it would not be surprising if smaller scale cooling flows occurred at earlier cosmological epochs since X-ray data already suggest that cooling flows evolve hierarchically to larger scales (Evrard 1990, Katz & White 1993).

These considerations prompted Ashman & Carr (1988) and Thomas & Fabian (1990) to consider the circumstances in which one could expect high-pressure quasi-static flows to occur at pregalactic and protogalactic epochs. The situation is best illustrated for the hierarchical clustering scenario, in which, as time proceeds, increasingly large gas clouds bind and virialize. The mass fraction of a cloud cooling quasi-statically is maximized when the cooling time t_c is comparable to the free-fall time t_f: Collapse does not proceed at all for $t_c \gg t_f$, whereas it is not quasi-static for $t_c \ll t_f$. In any particular variant of the hierarchical clustering scenario, one can specify the mass binding as

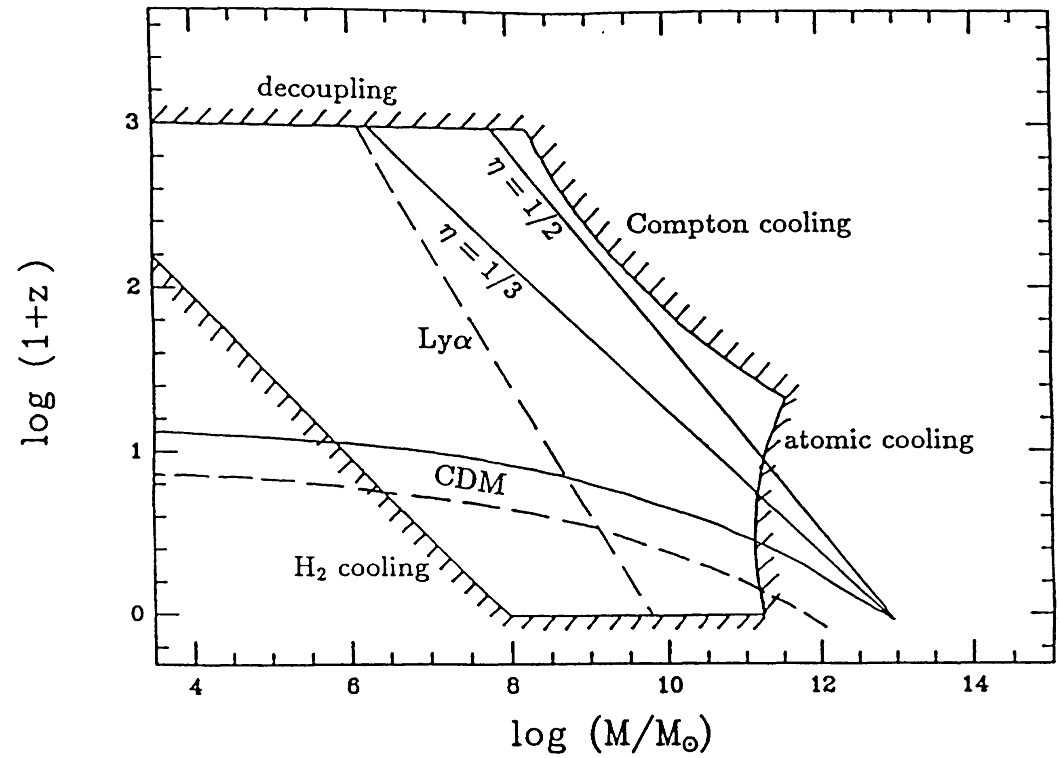

Figure 8 The (*M, Z*) region within which a cloud of mass *M* binding at a redshift *z* will cool within a Hubble time. The other lines show how the binding mass evolves with redshift for the CDM scenario with or without bias (*solid* and *broken lines*) and for the isocurvature model. A lot of gas may be processed through a cooling flow where the binding curve hits the cooling curve. This happens at both a pregalactic and protogalactic era in the CDM case, but the pressure is too low to make LMOs in the former case. In the isocurvature case, only protogalactic cooling flows occur.

a function of redshift. For a cloud of mass M, the dynamical time will just be of order the Hubble time at that redshift, whereas the cooling time will depend upon the density and virial temperature of the cloud (which are themselves determined by M and z). Thus, one can specify a region in the (M, z) plane of Figure 8 in which bound clouds will cool within a dynamical time. This applies above a lower mass limit associated with molecular hydrogen or Lyman-α cooling and below an upper mass limit associated with atomic hydrogen cooling (Rees & Ostriker 1977) or the Compton cooling of the microwave background.

The condition $t_c \sim t_f$ will be satisfied at the boundary of the region (shown shaded) and the intersection of this boundary with the binding curve $M(z)$ singles out two characteristic mass-scales and redshifts. These correspond to what Ashman & Carr term "Pervasive Pregalactic Cooling Flows" (PPCFs) and what Thomas & Fabian term "Maximal Cooling Flows" since the amount of gas cooling quasi-statically is maximized. The associated mass-scales are always of order 10^4–$10^8 M_\odot$ and $10^{11} M_\odot$, but the redshifts depend on the particular scenario. Figure 8 shows the binding curves corresponding to the Cold Dark Matter scenario, the broken curve corresponding to the biased version, and the baryon-dominated isocurvature scenario (with η specifying the exponent in the mass dependence of the density fluctuations at decoupling).

One might anticipate most of the dark matter being made on the smaller scale because much of the gas will have been consumed by the time atomic cooling becomes important. However, this does not happen in the Cold Dark Matter picture because the spectrum of fluctuations is very flat on subgalactic scales and, in the isocurvature models, $M(z)$ may never be small enough for low mass PPCFs to occur after decoupling. Both these features are indicated in Figure 8. Ashman & Carr (1992) therefore argue that most of the dark matter would need to be made by high mass protogalactic PPCFs. Another argument in favor of the protogalactic PPCFs is that the pressure is probably too low to make LMOs on the smaller scale.

One problem with invoking protogalactic cooling flows to make the dark matter is that one might expect most of the gas to have gone into clouds with $t_c < t_f$ and such clouds should make ordinary stars. This "cooling catastrophe" raises the question of whether there could be enough gas left over to make ordinary galaxies (White & Frenk 1991, Blanchard et al 1992). One way around this is to invoke supernovae to reheat the gas so that most of it can avoid cooling until the protogalactic epoch (Thomas & Fabian 1990). Another way is to argue that even clouds with $t_c < t_f$ can make a lot of dark matter (Ashman 1990). The idea here is that gas always drops out at such a rate as to preserve the PPCF condition $t_c \sim t_f$ for the surviving gas. One thus gets a two-phase medium, with cool dense clouds embedded in hot high-pressure gas. This was originally proposed as a mechanism to make globular clusters at a protogalactic epoch (Fall & Rees 1985), but Ashman (1990) argues that sufficiently small clouds would fragment into dark clusters rather than visible clusters in the presence of molecular hydrogen. By applying the same idea to other galaxies, he predicts that the fraction of dark mass in spirals should increase with decreasing disk mass and this may be observed (Persic & Salucci 1990).

9.3 *M-Dwarfs vs Brown Dwarfs*

In determining how small LMOs would need to be to provide the disk or halo dark matter, important information comes from red and infrared observations. From searches for sources in our own halo, Richstone et al (1992) find that the halo mass-to-light ratio from stars between $0.5M_\odot$ and $0.8M_\odot$ exceeds 400, while Bahcall & Soneira (1984) find that the ratio from stars down to $0.15M_\odot$ must exceed 650. This implies that stars in these mass ranges can only contribute a small fraction to the halo density. Even stronger constraints come from Gilmore & Hewett (1983), who find that the local number density of stars in the mass range 0.08–$0.1M_\odot$ can be at most 0.01 pc^{-3}. This is a hundred times too small to explain the local dark matter problem and ten times too small to explain the halo problem.

A similar conclusion is indicated by infrared observations of other spiral galaxies. For example, the K-band mass-to-light ratio exceeds 50 for NGC 4565 (Boughn et al 1981), 100 for M87 (Boughn & Saulson 1983), 64 for NGC 5907 (Skrutskie et al 1985), and 140 for NGC 100 (Casali & James 1994). Since the mass-to-light ratio is less than 60 for stars bigger than $0.08M_{\odot}$, the lower limit for hydrogen-burning (D' Antona & Mazzitelli 1985), this suggests that any hydrogen-burning stars are excluded. Lake (1992) has criticized some of these limits on the grounds that they involve attributing all the dynamical mass to the halo objects but the correction to the mass-to-light ratio for M87 and NGC 100 could hardly get it below 60. These observations therefore suggest that the halo dark matter must be in the form of brown dwarfs.

9.4 *Evidence from Population I and Population II*

Although it is difficult to observe brown dwarfs (BDs) themselves, one can study the IMF of stars in the mass range above the hydrogen-burning limit and infer whether its extrapolation would permit a lot of BDs. If one assumes that the IMF has the power-law form

$$\frac{dN}{dm} \sim m^{-x} \quad \text{for} \quad m_{\text{min}} < m < m_{\text{max}} \tag{9.1}$$

(at least over some mass range), then most of the mass is in the smallest stars for $x > 2$ and in the largest ones for $x < 2$. Determining the value of x in the LMO range is difficult, partly because obtaining the luminosity function is hard and partly because there are large uncertainties in the mass-luminosity relation as one approaches the hydrogen-burning limit. Nevertheless, there does now seem to be a convergence of opinion (Bessell & Stringfellow 1993).

Let us first consider the possibility that the disk dark matter (if it exists) is in the form of BDs. Early studies of the luminosity function for nearby stars (Reid & Gilmore 1982, Gilmore & Reid 1983, Gilmore et al 1985) suggested that the IMF is too shallow for BDs to have an interesting density. These results were initially contradicted by the results of Hawkins (1985) and Hawkins & Bessell (1988), who went to somewhat fainter magnitudes and claimed that the observations were consistent with an IMF which steepened enough to put all the dark mass in BDs. However, the data of Tinney et al (1992, 1993) make it quite clear that the IMF flattens off below 0.2 $M_{\odot}$ and, unless it rises again below $0.08M_{\odot}$, the contribution to the local dark matter must be small (Tinney 1993). This is also consistent with the results of Kroupa et al (1993), Comeron et al (1993), and Hu et al (1994). In particular Kroupa et al (1993), find $x = 2.7$ for $m > 1M_{\odot}$, $x = 2.2$ for $0.5 < m < 1M_{\odot}$, and $0.7 < x < 1.8$ for $0.08M_{\odot} < m < 0.5M_{\odot}$. This suggests that stars of $0.5M_{\odot}$ should dominate the disk density. BDs may dominate the number density but, unless the value of x changes below $0.08M_\odot$, they cannot contain more than 1% of the disk mass.

The situation is less clear-cut when one considers Population II stars. Richer et al (1991) claim that metal-poor globular clusters have $x = 3.6$ below $0.5M_\odot$ down to at least $0.14M_\odot$, while Richer & Falman (1992) claim that stars in the Galactic Spheroid have $x = 4.5 \pm 1.2$ in the same mass range. This does allow the possibility that most of the mass is in the smallest objects; indeed, BDs could explain all the halo dark matter if the IMF extended down to $M_{min} \sim 0.01M_\odot$. However, Richer & Falman also point out that the rotation curve of the Galaxy requires that the total spheroid mass cannot exceed $7 \times 10^{10}M_\odot$, which implies that the IMF cannot extend below $0.05M_\odot$. It is therefore unlikely that Population II stars themselves could explain the halo dark matter. As stressed by Lake (1992), the main point of these results is that they lend support to the suggestion that low metallicity enhances the fraction of mass in low mass objects.

It should be stressed that there is an important difference between attributing the disk and the halo dark matter to BDs. If the disk dark matter comprises BDs, one would expect them to represent the low mass tail of the Population I IMF since all disk stars presumably form at the same time. However, there may be no connection between the dark halo stars and Population II stars because they probably form at a different time and place. One should therefore be wary of attempts to exclude the halo from comprising BDs on the grounds that Population II stars have a particular IMF, as do Hegyi & Olive (1983, 1986, 1989).

9.5 *Infrared Searches for Brown Dwarfs*

Even though brown dwarfs do not burn hydrogen, they still generate some luminosity in the infrared. They radiate first by gravitational contraction (for about $10^7 y$) and then by degenerate cooling. If the disk or halo dark matter is in the form of brown dwarfs, it is therefore important to consider whether they can be detected via this infrared emission. Current constraints on BDs are rather weak (Low 1986, van der Kruit 1987, Beichmann et al 1990, Nelson et al 1993) but the prospects of detection will be much better with impending space satellites such as *ISO* and *SIRTF*.

The problem has been addressed in various contexts by several authors. Karimabadi & Blitz (1984) have calculated the expected intensity from BDs with a discrete IMF comprising an $\Omega = 1$ cosmological background. Adams & Walker (1990) have discussed the possibility of detecting the collective emission of the brown dwarfs in our own Galactic halo for both a discrete and power-law IMF. Daly & McLaughlin (1992) have considered the prospects of detecting the emission of individual halo brown dwarfs of a given mass and age in the Solar vicinity, as well as the collective emission of brown dwarfs in other galaxy halos.

Kerins & Carr (1994) have considered the possibility that the BDs are assembled into dark clusters and also discuss how infrared observations at different wavelengths could be used to probe the mass spectrum of the brown dwarfs.

As an illustration of the feasibility of detecting radiation from BDs, let us consider the prospects of detecting the nearest one in our halo. If the BDs all have the same mass m, then the local halo density ($\rho_o = 0.01 M_\odot \mathrm{pc}^{-3}$) implies that the expected distance to the nearest one is $0.55(m/0.01M_\odot)^{1/3}$pc. The expected spectra are shown in Figure 9 and compared to the sensitivities of *IRAS* and *ISO*. This assumes the temperature and luminosity of Stevenson (1986) where the BD age and opacity are taken to be 10^{10}y and 0.01 cm^{2}g^{-1} (corresponding to electron-scattering). Although *IRAS* gives no useful constraints (it is too weak by a factor of 2 even for the optimal mass of $0.07M_\odot$), the ISOCAM instrument on *ISO* could detect $0.08M_\odot$ BDs in a few hours, $0.04M_\odot$ BDs in a few days, and $0.02M_\odot$ BDs in a few months. Note that disk BDs, would be younger, locally more numerous, and more opaque than halo BDs, increasing the peak flux by 6 and decreasing the peak wavelength by 0.6. *IRAS* results

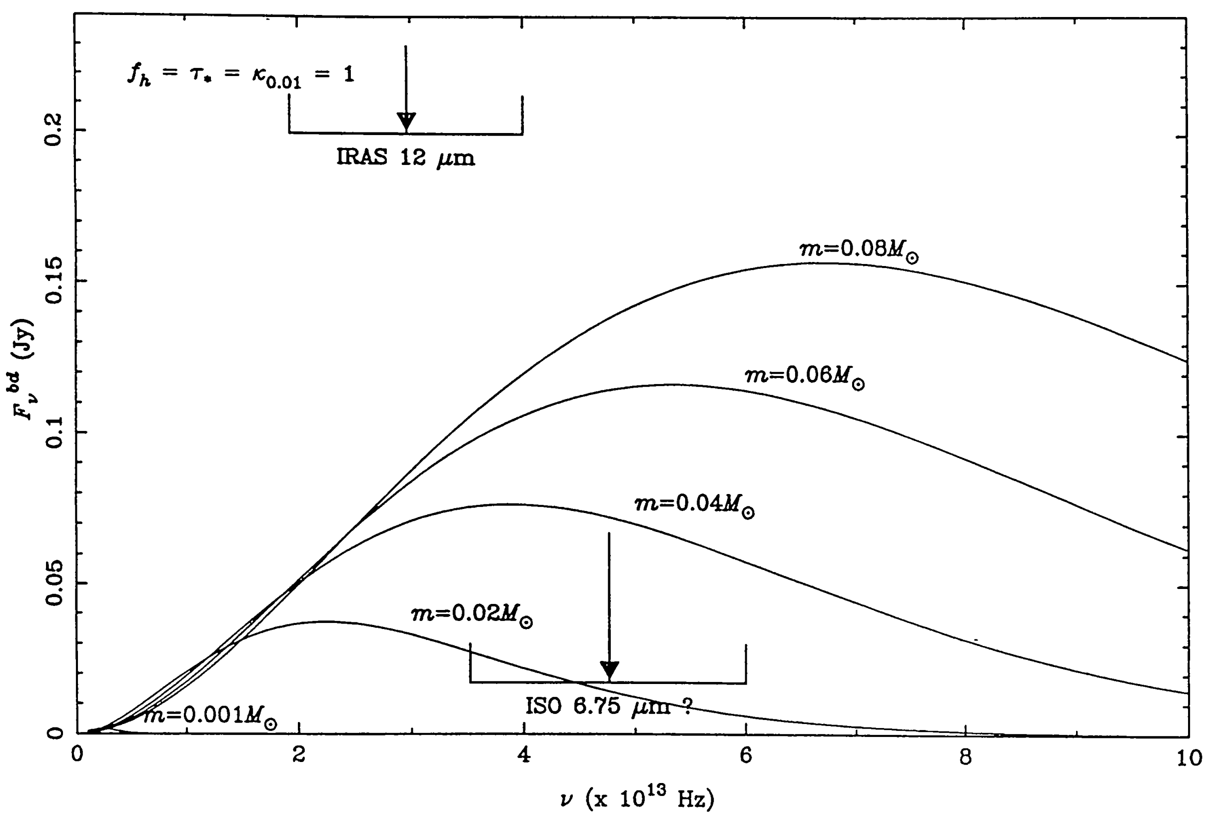

Figure 9 Expected flux from the nearest halo BD for various values of BD mass. The *IRAS* point source sensitivity at 12μ is shown; this is a factor of two above the predicted flux even in the optimal case. The expected 3σ *ISO* 6.75μ sensitivity is also shown, assuming an observation time of 10 days and a 100 s integration time.

already imply that BDs with a discrete IMF could provide the disk dark matter only if their mass is below $0.01 M_\odot$.

One might expect the BDs to be easier to detect if they are in clusters. This is because, although the distance to the nearest source is increased by a factor $(M_c/m)^{1/3}$, the luminosity is increased by (M_c/m), giving an increase in flux of $(M_c/m)^{1/3}$. Rix & Lake (1993) have already used this to exclude the cluster scenario. However, they assume that the clusters are point sources and, as illustrated in Figure 4, the dynamical constraints discussed in Section 6.4 imply that the clusters will always be extended sources. In fact, the *IRAS* extended source sensitivity (EES) at 12μ is too low to permit the detection of clusters. The *ISO* extended source sensitivity at 6.75μ will suffice, but the time required to find these clusters is very sensitive to their mass and radius. Note that the halo clusters will cover the sky if they are large enough, corresponding to the line $K_h > 1$ in Figure 4, in which case detecting the clusters is equivalent to detecting the halo background. *ISO* would take several months to detect the Galactic background, even in the optimal case with $m = 0.08 M_\odot$ (Kerins & Carr 1994). The background spectrum in this case is also indicated in Figure 6.

10. CONCLUSIONS AND FUTURE PROSPECTS

10.1 *Reappraisal of Baryonic Dark Matter Candidates*

By way of summarizing the key points of this review, and also because it provides an opportunity to mention some candidates that have not yet been covered, we conclude with a reappraisal of the various baryonic dark matter candidates (cf Carr 1990, Dalcanton et al 1994).

SNOWBALLS Condensations of cold hydrogen can be excluded in most mass ranges. In order to avoid being disrupted by collisions within the age of the Universe, they must have a mass of at least 1g (Hegyi & Olive 1983, Wollman 1992). Constraints in the mass range above this have been discussed by Hills (1986): Snowballs are excluded by the upper limit on the frequency of encounters with interstellar meteors between 10^{-3}g and 10^{7}g, by the number of impact craters on the Moon between 10^{7}g and 10^{16}g, and by the fact that no interstellar comet has crossed the Earth's orbit in the last 400 years between 10^{15}g and 10^{22}g. The limits are marginally stronger for halo objects, because of their larger velocities, and are shown in Figure 3. Hegyi & Olive (1983) have argued that snowballs would be evaporated by the microwave background, but Phinney (1985) has pointed out that this only happens below a mass of 10^{22}g. De Rujula et al (1992) have claimed an even stronger limit on the grounds that snowballs smaller than $10^{-7} M_\odot \sim 10^{26}$g would be evaporated within the age of the Universe by their own heat; this is also indicated in Figure 3. Another argument against snowballs is that, since one would expect only hydrogen to condense, the cosmic helium abundance would be increased to an unacceptably high value if the fraction of the Universe going into them were more than $(1 - Y_{\rm min}/Y_{\rm max})$, where $Y_{\rm min}$ is the minimum primordial abundance (≈ 0.2) and $Y_{\rm max}$ is the maximum presolar helium abundance (≈ 0.3). This suggests that the fraction must be less than 30%.

BROWN DWARFS Fragmentation could in principle lead to objects smaller than $0.08M_\odot$ and there may be evidence that such brown dwarfs form prolifically in cooling flows (Section 9.1). Such objects might be detectable as infrared sources; it is not surprising that *IRAS* has not found them but *ISO* or *SIRTF* could be expected to detect brown dwarfs with masses down to $0.01M_\odot$ (Section 9.5). Another important signature of brown dwarfs, in either our own or other galactic halos, is the intensity fluctuations in stars or quasars induced by their microlensing effects. This effect would be observable for objects over the entire brown dwarf mass range and may have already been found (Sections 7.2, 7.3, and 7.7). Observations of microlensing on different timescales could also give information about the mass spectrum of the brown dwarfs (De Rujula et al 1991). The brown dwarf scenario currently appears to be the most plausible. In any case, the combination of infrared and microlensing searches should soon either confirm or eliminate it.

M-DWARFS Stars in the range 0.3–0.8 $M_\odot$ are excluded from solving any of the dark matter problems by background light limits (Section 5.1). Lower mass hydrogen-burning stars would also seem to be excluded by source count constraints and infrared measurements of other galaxy halos (Section 9.3).

WHITE DWARFS These would be the natural end-state of stars with initial mass in the range of 0.8–$8M_\odot$ and they could certainly fade below detectability if they formed sufficiently early in the history of the Galaxy. The fraction of the original star that is left in the white dwarf remnant is low but one could still produce a lot of dark matter if there were many generations of stars (Larson 1986). In some sense white dwarfs are the most conservative candidates, since we know that they form prolifically today. The problem is that one needs a very contrived mass spectrum if they are presumed to make up galactic halos: The IMF must be restricted to between 2 and 8 $M_\odot$ to avoid producing too much light or too many metals (Ryu et al 1990) and even then one must worry about excessive helium production (Section 5.3). However, this scenario would have many interesting observational consequences, such as an abundance of cool white dwarfs (Tamanaha et al 1990) and a large number of X-ray sources formed from white dwarf binaries which have coalesced into neutron stars (Silk 1993). A potential problem is that the fraction of white dwarfs in binaries might produce too many type 1a supernovae (Smecker & Wyse 1991), although this might actually be required to explain the high-velocity pulsars moving towards the disk in our own Galaxy (Eichler & Silk 1992). Even if white dwarfs do not have a high enough density to explain the halo dark matter, they could still explain the dark matter in the Galactic disk (if this exists).

NEUTRON STARS Although neutron stars would be the natural end-state of stars in some mass range above 8 $M_\odot$, the fact that the poorest Population I stars have metallicity of order 10^{-3} places an upper limit on the fraction of the Universe's mass that can have been processed through the stellar precursors—this probably precludes their explaining any of the dark matter problems (Section 5.2). The only way out is to adopt the proposal of Wasserman & Salpeter (1993) in which the neutron stars are in clusters, so that their nucleosynthetic products are trapped within the cluster potentials. Even in this scenario, the neutron stars contain only 1% of the halo dark matter; most of the mass is in asteroids. Nevertheless, the small admixture of neutron stars has an intriguing consequence since collisions between the neutron stars and asteroids are supposed to explain gamma-ray bursts.

STELLAR BLACK HOLES Stars larger than some critical mass $M_{BH} \approx 25$–$50M_\odot$ may leave black hole rather than neutron star remnants, with most of their nucleosynthetic products being swallowed. However, they will still return a substantial amount of heavy elements through winds prior to collapsing (Maeder 1992), so normal stellar black holes are probably excluded. In any case, stellar black holes could not provide the disk dark matter because the survival of binaries in the disk requires that the local dark objects are smaller than $2M_\odot$ (Section 6.5). Stellar black holes could also be detected by their lensing effects on the line-to-continuum ratio of quasars; this already excludes black holes from having a critical density below $300M_\odot$ or a tenth critical density (required for halos) below $20M_\odot$ (Section 7.5).

VMO BLACK HOLES Since stars larger than some critical mass $M_c \approx 200M_\odot$ undergo complete collapse, they may be better candidates for the dark matter than ordinary stars. However, VMOs are radiation-dominated and therefore unstable to pulsations; these pulsations are unlikely to be completely disruptive, but they could lead to considerable mass loss and possible overproduction of helium (Section 5.3). Another important constraint on the number of stellar black hole remnants is provided by background light limits. Although these can be obviated if the stars burn at a sufficiently high redshift, the scenario is becoming increasingly squeezed by the *FIRAS* data (Section 8.2). However, VMO black holes are relatively unconstrained by lensing effects, since the line-to-continuum constraint only applies below $300M_\odot$ (Section 7.5). Laser interferometry might just detect the gravitational wave background generated by a large population of VMO black holes, especially if they form in binary systems (Section 8.4).

SUPERMASSIVE BLACK HOLES We have seen that SMOs larger than $10^5 M_\odot$ would collapse directly to black holes without any nuclear burning due to relativistic instabilities. However, halo black holes would heat up the disk stars more than is observed unless they were smaller than about $10^6 M_\odot$ (Section 6.1), so they would have to lie in the narrow mass range 10^5–$10^6 M_\odot$, and the survival of globular clusters (Section 6.2) and dynamical friction effects (Section 6.3) probably exclude even this range. If the dark matter in clusters comprises black holes, then the absence of unexplained tidal distortions in the visible galaxies implies that they must be smaller than $10^9 M_\odot$ (Section 6.5). The number of SMO black holes is also constrained by macrolensing searches: Their density parameter must be less than 0.4 between 10^7 and $10^9 M_\odot$ and less than 0.02 between 10^{11} and $10^{13} M_\odot$ (Section 7.2). The background gravitational waves generated by the formation of SMO black holes could in principle be detected by space interferometers or the Doppler tracking of interplanetary spacecraft (Section 8.4).

10.2 *Best Bet Candidates*

The various constraints on the form of baryonic dark matter discussed in this review are brought together in Table 2; the shaded regions are excluded by either dynamical, nucleosynthetic, lensing, or light constraints. This assumes that the objects all have the same mass, so that one does not have extra constraints associated with assumptions about the IMF. The dotted regions may also be excluded but this is less certain. Table 2 does not include the dynamical constraints on the nonbaryonic candidates, but it should be noted that only cold inos could explain the presence of dark matter in galaxies. However, hot inos could explain the cluster and background dark matter; large-scale structure and microwave anisotropy observations may even require a mixture of hot and cold inos (Taylor & Rowan Robinson 1992).

Whether the dotted region in Table 2 is excluded depends on whether one believes that the primordial nucleosynthesis constraint permits the cluster dark matter to be baryonic. This is possible only if one invokes inhomogeneous cosmological nucleosynthesis, but this scenario should still be taken seriously. It would be remarkable if the Universe came through the quark hadron phase transition with no fluctuations at all; the surprise is that the resulting light element abundance are relatively insensitive to these. On the other hand, it seems clear that even inhomogeneous nucleosynthesis will not permit baryons to have the critical density. A critical baryon density is excluded in most mass ranges anyway. The prospects for the "maximal BDM" scenario therefore seem bleak.

The prime message of Table 2 is that one could not expect any single candidate to explain all four dark matter problems. On the other hand, the table does constrain the possible solutions:

Table 2 Constraints on baryonic dark matter candidates[a]

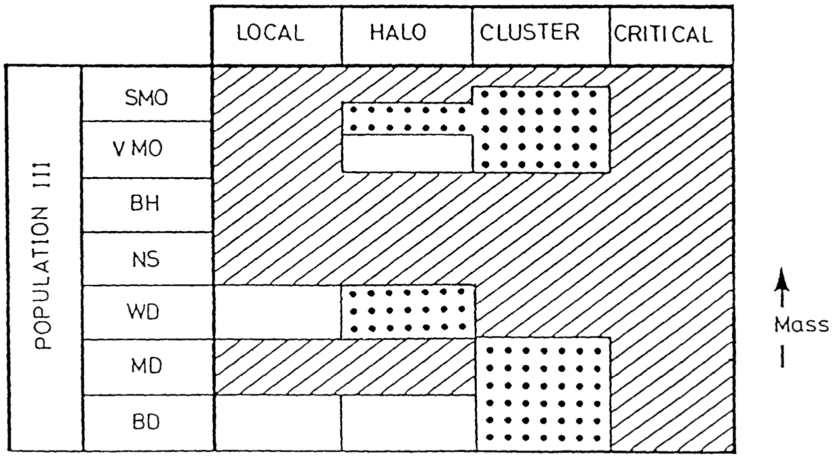

[a]The shaded regions are excluded by at least one of the limits discussed in the text and the dotted regions are improbable. SMO, VMO, and BH refer to the black hole remnants of Supermassive Objects, Very Massive Objects, and ordinary stars respectively; WD = white dwarf; MD = M-dwarf; BD = brown dwarf.

1. The local dark matter (if it exists) could be white dwarfs or brown dwarfs but observations of the Population I IMF gives no reason for expecting this; presumably it could not be inos since these are nondissipative and so would not settle into a disk.

2. The halo dark matter could be brown dwarfs, white dwarfs, or VMO black holes; all of these possibilities require a departure from the standard Population II IMF, but the first probably requires the least radical departure since observations may already indicate a preponderance of low mass stars at small metallicity (white dwarfs—although in a sense the most conservative candidate—require cutting the IMF off at both ends).

3. The cluster dark matter may be partly baryonic, especially if galactic halos are baryonic, but we have seen that it could only be dominated by baryonic dark matter if one invokes inhomogeneous cosmological nucleosynthesis.

4. The background dark matter (if it exists) would have to be inos; if the inos are cold, one would expect both the halo and cluster dark matter to be a mixture of WIMPs and MACHOs.

Finally, we should comment on the possibility of Primordial Black Holes (PBHs). Although these are not baryonic (since they form mainly from radiation rather than from gas), they share many of the features of their baryonic counterparts. These could certainly contribute to the dark matter in principle, and those smaller than $10^5 M_\odot$ (which form before the time of cosmological nucleosynthesis) could have the critical density. However, whether they form from initial inhomogeneities (Hawking 1971, Carr 1975), from phase transitions (Hawking et al 1982, Crawford & Schramm 1982, Dolgov & Silk 1993), or from the collapse of cosmic loops (Polnarev & Zemboricz 1988, Hawking 1989), fine-tuning is required to get an interesting cosmological density because the fraction of the Universe going into PBHs at time t must be $\sim 10^{-6} t^{1/2}$, where t is in seconds. Therefore, despite the invocation of PBHs to explain gravitational lensing effects (Section 7.3), this does not seem very likely.

10.3 *Future Prospects*

Some of the most exciting developments in this field have come from gravitational lensing studies and we can expect a proliferation of these efforts in the next few years. Macrolensing searches are placing ever more stringent limits of the number of high mass baryonic objects; microlensing searches may have already provided evidence for low mass ones. It is surely significant that microlensing evidence from both quasars and stars all point towards lens masses in the range 0.001–$0.1 M_\odot$. Admittedly, the masses indicated by the MACHO and EROS results are marginally too high; the most likely values are all in the M-dwarf range, whereas light constraints require the halo objects to be smaller than $0.08 M_\odot$. Nevertheless, there is a fairly broad probability distribution for the lensing masses, depending on the assumed velocity and spatial distribution of the halo objects (Kerins 1994), so this puzzle may yet be resolved.

Although we have not reviewed here the plethora of theoretical papers that have appeared since the microlensing results were announced, it should be stressed that, even if the lensing results are genuine, they do not preclude WIMPs from providing some or even most of the dark halo. This is because the microlensing searches only probe the part of the halo at Galactocentric radii from 10–20 kpc, whereas the halo itself could extend much further than this. There could therefore be plenty of WIMPs further out, especially if the dark baryons are preferentially concentrated as a result of dissipation. Even within the 10–20 kpc region, the number of MACHO and EROS events observed merely suggests that the fraction of halo mass in MACHOs must exceed 10% (Gates & Turner 1994). It is therefore important that WIMP searchers should not be too discouraged by the success of the MACHO searchers. It still seems a fair bet that the world needs both MACHOs and WIMPs.

Another source of exciting developments in this field has been *COBE*. We have seen that the *FIRAS* constraints on the microwave spectral distortions and the *DIRBE* measurements of the infrared background density already severely restrict any scenario in which the dark matter is in the relics of massive stars. This is especially true if the radiation has been reprocessed into the far-IR by dust. Indeed, the only hope for these scenarios may be that the radiation remains in the near-IR where it may be hidden by interplanetary dust emission. The *FIRAS* constraints on the Compton y-parameter may also exclude the supermasive accreting black hole scenario. The *COBE* DMR constraints on the microwave anisotropies (though not treated in detail here) are also highly pertinent to the baryonic dark matter scenarios. Some people claim that these already rule out baryon-dominated models, but this conclusion is sensitive to assumptions about the form of the initial density fluctuations, so this has not been stressed here.

Looking further to the future, two more developments will have an important impact. If the halo dark matter is in brown dwarfs, then the next generation of infrared space satellites will either detect these or push their mass down to below $0.001 M_\odot$. In this case, we have stressed the importance of knowing whether the brown dwarfs are clustered because this determines whether one is seeking discrete or extended sources. If the halo dark matter is in black holes, then the next generation of gravitational wave detectors (either ground-based or space-based interferometers) will have an excellent chance of detecting the associated gravitational radiation—the period and amplitude of the waves will indicate the mass and formation redshift of the black holes. It seems likely that MACHOS will have been identified or excluded by the end of the millenium!

ACKNOWLEDGMENTS

Much of my own work over the past decade has focused on the topic of this review, so I hope my own prejudices have not shown too glaringly. I would like to thank all my baryonic-dark-matter collaborators over this period for many enjoyable and stimulating interactions: Dave Arnett, Keith Ashman, Bruno Bertotti, Dick Bond, Wolfgang Glatzel, Craig Hogan, Satoru Ikeuchi, Eamonn Kerins, Cedric Lacey, Jonathan McDowell, Joel Primack, Martin Rees, Michael Rowan-Robinson, Mary Sakellariadou, Humitako Sato, Joe Silk, and Mike Turner. I would also like to thank Cathy Clarke, Andy Fabian, Gerry Gilmore, Mike Hawkins, George Lake, Ben Moore, Adi Nusser, Bernard Pagel, and Sasha Polnarev for helpful discussions. Finally, I would like to thank Eamonn Kerins for helping me in my literature search and Jonathan Gilbert for his assistance in producing the figures.

Literature Cited

Aaronson M. 1983. *Ap. J. Lett.* 266:L11
Aaronson M, Olszewski E. 1987. In *Dark Matter in the Universe,* ed. J Kormendy, GR Knapp, p. 153. Dordrecht:Reidel
Adams FC, Freese K, Levin J, McDowell J. 1989. *Ap. J.* 360:24
Adams FC, Walker TP. 1990. *Ap. J.* 359:57
Alcock C, Fuller GM, Mathews GJ. 1987. *Ap.*

J. 320:439
Alcock C, Akerlof CW, Allsman RA, Axelrod TS, Bennett DP, et al. 1993. *Nature* 365:621
Applegate JH, Hogan CJ, Scherrer RJ. 1987. *Phys. Rev. D* 35:1160
Arnett WD. 1978. *Ap. J.* 219:1008
Arp HC, Burbidge G, Hoyle F, Narlikar JV, Wickramasinghe NC. 1990. *Nature* 346:807
Ashman KA. 1990. *MNRAS* 247:662
Ashman KA. 1992. *Publ. Astron. Soc. Pac.* 104:1109
Ashman KM, Carr BJ. 1988. *MNRAS* 234:219
Ashman KM, Carr BJ. 1991. *MNRAS* 249:13
Ashman KM, Salucci P, Persic M. 1993. *MNRAS* 260:610
Auborg E, Bareyre P, Bréhin S, Gros M, Lachièze-Ray M, et al. 1993. *Nature* 365:623
Babul A, Katz N. 1993. *Ap. J. Lett.* 406:L51
Bahcall JN. 1984a. *Ap. J.* 276:156
Bahcall JN. 1984b. *Ap. J.* 276:169
Bahcall JN. 1984c. *Ap. J.* 287:926
Bahcall JN, Flynn C, Gould A. 1992a. *Ap. J.* 389:234
Bahcall JN, Hut P, Tremaine S. 1985. *Ap. J.* 290:15
Bahcall JN, Soneira RM. 1984. *Ap. J. Suppl.* 55:67
Bahcall JN, Maoz D, Doxsey R, Schneider DP, Bahcall NA, et al. 1992b. *Ap. J.* 387:56
Barcons X, Fabian AC, Rees MJ. 1991. *Nature* 350:685
Bartleman M, Schneider P. 1993. *Astron. Astrophys.* 268:1
Beers TC, Preston GW, Shectman SA. 1992. *Astron. J.* 103:1987
Begelman MC, Blandford RD, Rees MJ. 1980. *Nature* 287:307
Beichman CA, Chester T, Gillett FC, Low FJ, Matthews K, Neugebauer G. 1990. *Astron. J.* 99:1569
Bertotti B, Carr BJ. 1980. *Ap. J.* 236:1000
Bertschinger E. 1983. *Ap. J.* 268:17
Bertschinger E, Dekel A. 1989. *Ap. J. Lett.* 336:L5
Bessel MS, Norris J. 1984. *Ap. J.* 285:622
Bessel MS, Stringfellow GS. 1993. *Annu. Rev. Astron. Astrophys.* 31:433
Bienayme O, Robin AC, Creze M. 1987. *Astron. Astrophys.* 180:94
Blaes OM, Webster RL. 1992. *Ap. J. Lett.* 391:L63
Blanchard A, Valls-Gabaud D, Mamon GA. 1992. *Astron. Astrophys.* 264:365
Blandford RD, Jaroszynski M. 1981. *Ap. J.* 246,1
Blandford RD, Narayan R. 1992. *Annu. Rev. Astron. Astrophys.* 30:311
Blandford RD, Rees MJ. 1991. In *Testing the AGN Paradigm,* ed. S Holt, S Neff, C Urry, p. 3. Woodbury, NY:Am. Inst. Phys.
Blitz L, Spergel DN. 1991. *Ap. J.* 370:205
Blumenthal GR, Faber SM, Flores R, Primack JR. 1986. *Ap. J.* 301:27
Blumenthal GR, Faber SM, Primack JR, Rees MJ. 1984. *Nature* 311:517
Bond HE. 1981. *Ap. J.* 248:606
Bond JR, Arnett WD, Carr BJ. 1984. *Ap. J.* 280:825
Bond JR, Carr BJ. 1984. *MNRAS* 207:585
Bond JR, Carr BJ, Arnett WD. 1983. *Nature* 304:514
Bond JR, Carr BJ, Hogan CJ. 1986. *Ap. J.* 306:428
Bond JR, Carr BJ, Hogan CJ. 1991. *Ap. J.* 367:420
Bond JR, Efstathiou G, Silk J. 1980. *Phys. Rev. Lett.* 45:1980
Bosma A. 1991. In *Warped Disks and Inclined Rings Around Galaxies,*, ed. S Casertano, PD Sackett, F Briggs, p. 40. Provo:Brigham Young Univ. Press
Boughn SP, Saulson PR. 1983. *Ap. J. Lett.* 265:L55
Boughn SP, Saulson PR, Seldner M. 1981. *Ap. J. Lett.* 280:L15
Bristow P, Phillipps S. 1994. *MNRAS* 267:13
Boyle BL, Fong R, Shanks T. 1988. *MNRAS* 231:897
Burstein D, Haynes MP, Faber SM. 1991. *Nature* 353:515
Canizares C. 1981. *Nature* 291:620
Canizares CR. 1982. *Ap. J.* 263:508
Carignan C, Beaulieu S, Freeman KC. 1990. *Astron. J.* 99:178
Carignan C, Freeman KC. 1988. *Ap. J. Lett.* 332:L33
Carlberg RG, Dawson PC, Hsu T, VandenBerg DD. 1985. *Ap. J.* 294:674
Carr BJ. 1975. *Ap. J.* 201:1
Carr BJ. 1978. *Comm. Astrophys.* 7:161
Carr BJ. 1979. *MNRAS* 189:123
Carr BJ. 1981a. *MNRAS* 195:669
Carr BJ. 1981b. *MNRAS* 194:639
Carr BJ. 1990. *Comm. Astrophys.* 14:257
Carr BJ, Bond JR, Arnett WD. 1984. *Ap. J.* 277:445
Carr BJ, Ikeuchi S. 1985. *MNRAS* 213:497
Carr BJ, Lacey CG. 1987. *Ap. J.* 316:23
Carr BJ, Rees MJ. 1984. *MNRAS* 206:315
Carr BJ, Sakellariadou M. 1994. Preprint
Casali M, James P. 1994. *MNRAS* In press
Cayrel R. 1987. *Astron. Astrophys.* 168:81
Cen RY, Ostriker JP, Peebles PJE. 1993. *Ap. J.* 415:423
Cen RY, Ostriker JP, Spergel DN, Turok N. 1991. *Ap. J.* 383:1
Chandrasekhar S. 1964. *Ap. J.* 140:417
Chiba T, Sugiyama N, Suto Y. 1993. Preprint
Coles P, Ellis. GFR. 1994. *Nature* In press
Comeron F, Rieke GH, Burrows A, Rieke M. 1993. *Ap. J.* 416:185
Corrigan RT, Irwin MJ, Arnaud J, Fahlman GG, Fletcher JM, et al. 1991. *Astron. J.* 102:34
Crampton D, McClure RD, Fletcher JM, Hutchings JB. 1989. *Astron. J.* 98:1188
Crawford M, Schramm DN. 1982. *Nature*

298:538
Dalcanton J, Canizares C, Granados A, Steidel CC, Stocke JT. 1994. *Ap. J.* In Press
Daly RA, McLaughlin GC. 1992. *Ap. J.* 390:423
D'Antona F, Mazzitelli I. 1985. *Ap. J.* 296:502
de Araujo JCN, Opher R. 1990. *Ap. J.* 350:502
Dekel A, Rees MJ. 1987. *Nature* 326:455
De Rujula A, Jetzer Ph, Masso E. 1991. *MNRAS* 250:348
De Rujula A, Jetzer Ph, Masso E. 1992. *Astron. Astrophys.* 254:99
de Zeeuw PT. 1992. In *Morphological and Physical Classification of Galaxies,* ed. G Busarello, M Capacciolli, G Longo. Dordrecht:Kluwer
Disney M, Davies JI, Phillipps S. 1989. *MNRAS* 239:939
Dolgov A, Silk J. 1993. *Phys. Rev. D* 47:4244
Draine BT, Shapiro PR. 1989. *Ap. J. Lett.* 344:L45
Dressler A, Faber SM, Burstein D, Davies RL, Lynden-Bell D, Terlevich RL, Wegner G. 1987. *Ap. J. Lett.* 313:L37
Dubinski J, Carlberg RG. 1991. *Ap. J.* 378:496
Efstathiou G. Bond JR, White SDM. 1992. *MNRAS* 258:1
Eichler D, Silk J. 1992. *Science* 257:937
Ellis GFR. 1988. *Class. Quant. Grav.* 5:891
Ellis GFR, Lythe DH, Mijic MB. 1991. *Phys. Lett. B* 271:52
Evrard AE. 1990. *Ap. J.* 363:349
Faber SM, Gallagher JS. 1979. *Annu. Rev. Astron. Astrophys.* 17:135
Fabian AC. 1994. *Annu. Rev. Astron. Astrophys.* 32:277
Fabian AC, Nulsen PEJ, Canizares CR. 1984. *Nature* 310:733
Fabian AC, Thomas PA, Fall SM, White RE. 1986. *MNRAS* 221:1049
Fall SM, Efstathiou G. 1981. *MNRAS* 193:189
Fall SM, Pei YC, McMahon RG. 1989. *Ap. J. Lett.* 341:L5
Fall SM, Rees MJ. 1977. *MNRAS* 81:37P
Fall SM, Rees MJ. 1985. *Ap. J.* 298:18
Fich M, Tremaine S. 1991. *Annu. Rev. Astron. Astrophys.* 29:409
Flores R, Primack JR, Blumenthal GR, Faber SM. 1993. *Ap. J.* 412:443
Forman W, Jones C, Tucker W. 1985. *Ap. J.* 293:102
Fowler W. 1966. *Ap. J.* 144:180
Fowler W. 1990. See Lynden-Bell & Gilmore 1990, p. 257
Fowler W, Hoyle F. 1964. *Ap. J. Suppl.* 9:201
Frenk CS, White SDM, Davis M, Efstathiou G. 1988. *Ap. J.* 327:507
Fricke KJ. 1973. *Ap. J.* 183:941
Fuller GM, Woosley SE, Weaver TA. 1986. 307:675
Garrett MA, Calder RJ, Porcas RW, King LJ, Walsh D, Wilkinson PN. 1994. *MNRAS* In press
Gates E, Turner MS. 1994. *Phys. Rev. Lett.* 72:2520
Gilmore G, Hewett P. 1983. *Nature* 306:669
Gilmore G, Reid N. 1983. *MNRAS* 202:1025
Gilmore G, Reid N, Hewett P. 1985. *MNRAS* 213:257
Glatzel W, El Eid MF, Fricke KJ. 1985. *Astron. Astrophys.* 149:419
Gnedin NYu, Ostriker JP. 1992. *Ap. J.* 400:1
Gnedin NYu, Ostriker JP, Rees MJ. 1994. *Ap. J.* In press
Gomez AE, Delhaye J, Grenier S, Jaschek C, Arenou F, Jaschek M. 1990. *Astron. Astrophys.* 236:95
Gott JR. 1981. *Ap. J.* 243:140
Gouda N, Sugiyama N. 1992. *Ap. J. Lett.* 395:L59
Gould A. 1990. *MNRAS* 244:25
Gould A. 1992. *Ap. J. Lett.* 386:L5
Griest K. 1991. *Ap. J.* 366:412
Guth AH. 1981. *Phys. Rev. D* 23:347
Haehnelt MG. 1994. *MNRAS* In press
Hammer F, LeFevreo. 1990. *Ap. J.* 357:38
Harrison ER. 1993. *Ap. J. Lett.* 405:L1
Hartquist T, Cameron AGW. 1977. *Astrophys. Space Sci.* 48:145
Hatsukade I. 1989. PhD thesis. Miyazaki Univ.
Hauser MG, Kelsall T, Moseley SH, Silverberg RF, Murdock T, et al. 1991. In *After the First Three Minutes,* ed. S Holt, C Bennet, V Trimble, p. 161. Woodbury, NY: Am. Inst. Phys.
Hawking SW. 1971. *MNRAS* 152:75
Hawking SW. 1989. *Phys. Lett. B* 231:237
Hawking SW, Moss IG, Stewart JM. 1982. *Phys. Rev. D* 26:2681
Hawkins I, Wright EL. 1988. *Ap. J.* 324:46
Hawkins MRS. 1985. *Phil. Trans. R. Astron. Soc.* 320:553
Hawkins MRS. 1993. *Nature* 366:242
Hawkins MRS, Bessell MS. 1988. *MNRAS* 234:177
Heflin MB, Gorenstein MV, Lawrence CR, Burke BF. 1991. *Ap. J.* 378:519
Hegyi DJ, Kolb EW, Olive KA. 1986. *Ap. J.* 300:492
Hegyi DJ, Olive KA. 1983. *Phys. Lett. B.* 126:28
Hegyi DJ, Olive KA. 1986. *Astrophys. J.* 303:56
Hegyi DJ, Olive KA. 1989. *Astrophys. J.* 346:648
Heisler J, Ostriker JP. 1988. *Ap. J.* 332:543
Henstock DR, Wilkinson PN, Browne IWA, Patnaik AR, Taylor GB, et al. 1993. In *Gravitational Lenses in the Universe*, ed. J Surdej, D Fraipent-Caro, E Gosset, S Refsdal, M Remy, p. 325. Univ. Liege.
Hewett PC, Webster RL, Harding ME, Jedrezewski RI, Foltz CB. 1989. *Ap. J. Lett.* 346:L61
Hewitt JN. 1986. PhD thesis. Mass. Inst. Technol. Cambridge
Hewitt JN, Burke BF, Turner EL, Schneider DP, Lawrence CR, et al. 1989. In *Gravitational Lenses,* ed. JM Moran, JN Hewitt, KY Loh, p. 147. Berlin:Springer-Verlag

Hills JG. 1986. *Astron. J.* 92:595
Hogan CJ. 1978. *MNRAS* 185:889
Hogan CJ. 1993. *Ap. J. Lett.* 415:L63
Hogan CJ, Narayan R, White SDM. 1989. *Nature* 339:106
Hogan CJ, Rees MJ. 1988. *Phys. Lett. B* 205:228
Hoyle F, Wickramasinghe NC. 1989. *Astrophys. Space Sci.* 154:143
Hu EM, Huang JS, Gilmore G, Cowie LL. 1994. *Nature* In press
Huchra J, Brodie J. 1987. *Astron. J.* 93:779
Hut P, Rees MJ. 1992. *MNRAS* 259:27P
Ikeuchi S. 1981. *Publ. Astron. Soc. Jpn.* 33:211
Ipser JR, Price RH. 1977. *Ap. J.* 216:578
Ipser JR, Semenzato R. 1985. *Astron. Astrophys.* 149:408
Irwin MJ, Webster RL, Hewett PC, Corrigan RT, Jedrzewski RI. 1989. *Astron. J.* 98:1989
Jin L. 1989. *Ap. J.* 337:603
Jin L. 1990. *Ap. J.* 356:501
Kaiser N. 1984. *Ap. J. Lett.* 284:L9
Kajino T, Mathews GJ, Fuller GM. 1990. *Ap. J.* 364:7
Karimabadi H, Blitz L. 1984. *Ap. J.* 283:169
Kashlinsky A, Rees MJ. 1983. *MNRAS* 205:955
Kassiola A, Kovner I, Blandford RD. 1991. *Ap. J.* 381:6
Katz N, White SDM. 1993. *Ap. J.* 412:455
Kayser R, Refsdal S, Stabell R. 1986. *Astron. Astrophys.* 166:36
Kerins E. 1994. Preprint
Kerins E, Carr BJ. 1994. *MNRAS* 266:775
Knapp GR. 1988. In *The Mass of the Galaxy,* ed. M. Fich, p. 35. CITA Workshop
Kovner I. 1991. *Ap. J.* 376:70
Krauss LM, Small TA. 1991. *Ap. J.* 378:22
Kronberg PP, Dyer CC, Burbidge EM, Junkkarinen VT. 1991. *Ap. J. Lett.* 367:L1
Kroupa P, Tout CA, Gilmore G. 1993. *MNRAS* 262:545
Kuijken K, Gilmore G. 1989. *MNRAS* 239:571,605,651
Kuijken K, Gilmore G. 1991. *Ap. J. Lett.* 367:L9
Kurki-Suonio H, Matzner RA, Olive KA, Schramm DN. 1990. *Ap. J.* 353:406
Lacey CG. 1991. In *Dynamics of Disk Galaxies,* ed. B Sundelius, p 257. Göteborg
Lacey CG, Field G. 1988. *Ap. J. Lett.* 330:L1
Lacey CG, Ostriker JP. 1985. *Ap. J.* 299:633
Lake G. 1990. *Ap. J. Lett.* 356:L43
Lake G. 1992. In *Trends in Particle Astrophysics,* ed. D. Cline, R. Peccei. World Scientific
Lake G, Schommer RA, van Gorkom JH. 1990. *Astron. J.* 99:547
Lange AE, Richards PL, Hayakawa S, Matsumoto T, Matsuo H, et al. 1991. Preprint
Lanzetta KM, Wolf AM, Turnshek DA, Lu LM, McMahon RG, Hazard C. 1991. *Ap. J. Suppl.* 77:1
Larson R. 1986. *MNRAS* 218:409
Latham DW, Tonry J, Bahcall JN, Soneira RM, Schechter PS. 1984. *Ap. J. Lett.* 281:L41
Layzer D, Hively RM. 1973. *Ap. J.* 179:361
Lewis GF, Miralda-Escude J, Richardson DC, Wambsganss J. 1993. *MNRAS* 261:647
Lin DNC, Faber SM. 1983. *Ap. J. Lett.* 266:L21
Linder EV, Schneider P, Wagoner RV. 1988. *Ap. J.* 324:786
Loeb A. 1993. *Ap. J.* 403:542
Loeb A, Rasio F. 1993. Preprint
Low FJ. 1986. In *Astrophysics of Brown Dwarfs,* ed. MC Kafatos, RS Harrington, SP Maran, p. 66. Cambridge:Cambridge Univ. Press
Low C, Lynden-Bell D. 1976. *MNRAS* 176:367
Lynden-Bell D, Gilmore G. 1990. *Baryonic Dark Matter.* Dordrecht:Kluwer
Maeder A. 1992 *Astron. Astrophys.* 264:105
Malaney RA, Fowler WA. 1988. *Ap. J.* 333:14
Malaney P, Mathews G. 1993. *Phys. Rep.* 229:147
Mao S. 1992. *Ap. J. Lett.* 389:L41
Matsumoto T, Akiba M, Murakami H. 1988b. *Ap. J.* 332:575
Matsumoto T, Hayakawa S, Matsuo H, Murakami H, Sato S, et al. 1988a. *Ap. J.* 329:567
Mather JC, Cheng ES, Eplee RE, Isaacman RB, Meyer SS, et al. 1990. *Ap. J. Lett.* 354:L37
Mather JC, Cheng ES, Cottingham DA, Eplee RE, Fixen DJ, et al. 1994. *Ap. J.* 420:439
Mathews GJ Schramm DN, Meyer BS. 1993. *Ap. J.* 404:476
Mateo M. Olszewski E, Welch DL, Fischer P, Kunkel W. 1991. *Astron. J.* 102:914
McDonald JM, Clarke CJ. 1993. *MNRAS* 262:800
McDowell JC. 1986. *MNRAS* 223:763
McGaugh S. 1994. *Nature* 367:538
Meszaros P. 1975. *Astron. Astrophys.* 38:5
Moore B. 1993. *Ap. J. Lett.* 413:L93
Moore B, Silk J. 1994. Preprint
Mould JR, Oke JB, de Zeeuw PT, Nemec JM. 1990. *Astron. J.* 245:454
Mulchaey JS, Davis DS, Mushotzky RF, Burstein D. 1993. *Ap. J. Lett.* 404:L9
Najita J, Silk J, Wachter JW. 1990. *Ap. J.* 348:383
Narayan R, Wallington S. 1992. *Ap. J.* 399:368
Negroponte J. 1986. *MNRAS* 222:19
Nelson LA, Rappaport SA, Joss PC. 1993 *Ap. J.* 404:723
Nemiroff RJ. 1989. *Ap. J.* 341:579
Nemiroff RJ. 1991a. *Comm. Astrophys.* 15:139
Nemiroff RJ. 1991b. *Phys. Rev. Lett.* 66:538
Nemiroff RJ, Bistolas V. 1990. *Ap. J.* 358:5
Nemiroff RJ, Norris JP, Wickramasinghe WADT, Horack JM, Kouveliotou C, et al. 1993. *Ap. J.* 414:36
Noda M, Christov VV, Matsuhara H, Matsumoto T, Matsuura S, et al. 1992. *Ap. J.* 381:456
Nottale L. 1986. *Astron. Astrophys.* 157:383
Nusser A, Dekel A. 1993. *Ap. J.* 405:437
Ober WW, El Eid MF, Fricke KL. 1983. *Astron. Astrophys.* 119:61
Oliver S, Rowan-Robison M, Saunders W. 1992.

MNRAS 256:15P
Oort J. 1932. *Bull. Astron. Inst. Neth.* 6:249
Ostriker JP, Cowie LL. 1981. *Ap. J. Lett.* 243:L127
Ostriker JP, Heisler J. 1984. *Ap. J.* 278:1
Ostriker JP, Binney J, Saha P. 1989. *MNRAS* 241:849
Ostriker JP, Peebles PJE, Yahil A. 1974. *Ap. J. Lett.* 193:L1
Ostriker JP, Vogeley MS, York DG. 1990. *Ap. J.* 364:405
Paczynski B. 1986. *Ap. J.* 304:1; 308:L43
Paczynski B. 1987. *Ap. J. Lett.* 317:L51
Pagel BEJ. 1987. In *The Galaxy,* ed. G Gilmore, B Carswell, p. 341. Dordrecht:Reidel
Pagel BEJ. 1990. See Lynden-Bell & Gilmore 1990, p. 237
Pagel BEJ. 1992. In *The Stellar Populations of Galaxies,* ed. B Barbuy, A Renzini. Dordrecht:Kluwer
Palla F, Salpeter EE, Stahler SW. 1983. *Ap. J.* 271:632
Patnaik AR, Browne IWA, Wilkinson PA, Wrobel JM. 1992. *MNRAS* 254:655
Peacock J. 1982. *MNRAS* 199:987
Peacock J. 1986. *MNRAS* 223:113
Peacock J, Dodds SJ. 1994. *MNRAS.* In Press
Peebles PJE. 1987a. *Nature* 237:210
Peebles PJE. 1987b. *Ap. J. Lett.* 315:L73
Peebles PJE, Dicke RH. 1968. *Ap. J.* 154:891
Peebles PJE, Partridge RB. 1967. *Ap. J.* 148:713
Persic M, Salucci P. 1990. *MNRAS* 245:257
Persic M, Salucci P. 1992. *MNRAS* 258:14P
Pfenniger D, Combes F, Martinet L. 1994. *Astron. Astrophys.* 285:79
Phinney ES. 1985. Preprint
Polnarev AG, Zemboricz R. 1988. *Phys. Rev. D* 43:1106
Ponman TJ, Bertram D. 1993. *Nature* 363:51
Press WH, Gunn JE. 1973. *Ap. J.* 185:397
Ramadurai S, Rees MJ. 1985. *MNRAS* 215:53P
Rana NC. 1991. *Annu. Rev. Astron. Astrophys.* 29:129
Rauch KP. 1991. *Ap. J.* 374:83
Rees MJ. 1976. *MNRAS* 176:483
Rees MJ. 1978. *Nature* 275:35
Rees MJ. 1984. In *Formation and Evolution of Galaxies and Large Structures in the Universe,* ed. J Audouze, J Tran Thanh Van, p. 271. Dordrecht:Reidel
Rees MJ. 1986. *MNRAS* 218:25P
Rees MJ, Ostriker JP. 1977. *MNRAS* 179:541
Refsdal S, Stabell R. 1991. *Astron. Astrophys.* 250:62
Reid N, Gilmore G. 1982. *MNRAS* 201:73
Richer HB, Fahlman GG. 1992. *Nature* 358:383
Richer HB, Fahlman GG, Buonanno R, Pecci FF, Searle L, Thompson IB. 1991. *Ap. J.* 381:147
Richstone D, Gould A, Guhathakurta P, Flynn C. 1992. *Ap. J.* 388:354
Rix H, Hogan CJ. 1988. *Ap. J.* 332:108
Rix H, Lake G. 1993. *Ap. J.* 417:1
Rodrigues-Williams LL, Hogan CJ. 1994. *Astron. J.* 107:451
Rowan-Robinson M. 1986. *MNRAS* 219:737
Rowan-Robinson M, Lawrence A, Saunders W, Crawford J, Ellis R, et al. 1990. *MNRAS* 247:1
Rubin VC, Ford WK, Thonnard N. 1980. *Ap. J.* 238:471
Ryu D, Olive KA, Silk J. 1990. *Ap. J.* 353:81
Sackett PD, Sparke LS. 1990. *Ap. J.* 361:408
Sakellariadou M. 1984. MS thesis. Cambridge Univ.
Salpeter EE. 1993. *Phys. Rep.* 227:309
Salpeter EE, Wasserman IM. 1993. Astron. Soc. Pac. 36:345.
Sancisi R, van Albada TS. 1987. In *Dark Matter in the Universe,* ed. J Kormendy, G Knapp, p. 67. Dordrecht:Reidel
Sarazin C. 1986. *Rev. Mod. Phys.* 58:1
Sargent WLW, Steidel CC. 1990. See Lynden-Bell & Gilmore 1990, p. 223
Saslaw WC, Narashima D, Chitre SM. 1985. *Ap. J.* 392:348
Saslaw WC, Valtonen MJ, Aarseth SJ. 1974. *Ap. J.* 190:253
Scaramella R, Bettolani G, Zamorani G. 1991. *Ap. J. Lett.* 376:L1
Scherrer RJ. 1993. *Ap. J.* 384:391
Schild H, Maeder A. 1985. *Astron. Astrophys. Lett.* 143:L7
Schneider DP, Schmidt M, Gunn JE. 1991. *Astron. J.* 102:837
Schneider P. 1993. *Astron. Astrophys.* 279:1
Schneider P, Ehlers J, Falco EE. 1992. In *Gravitational Lensing,* ed. R Kayser, T Schramm, L Nieser. Berlin:Springer-Verlag
Schneider P, Wagoner RV. 1987. *Ap. J.* 314:154
Schneider P, Weiss A. 1987. *Astron. Astrophys.* 171:49
Sellgren K, McGinn MT, Becklin EE, Hall DNB. 1990. *Ap. J.* 359:112
Shanks T. 1985. *Vistas Astron.* 28:595
Shu F, Adams F, Lizano S. 1987. *Annu. Rev. Astron. Astrophys.* 25:23
Silk J. 1968. *Ap. J.* 151:459
Silk J. 1977. *Ap. J.* 211:638
Silk J. 1991. *Science* 251:317
Silk J. 1992. In *The Stellar Populations of Galaxies,* ed. B Barbuy, A Renzini, p. 15. Dordrecht:Kluwer
Silk J. 1993. *Phys. Rep.* 227:143
Silk J, Stebbins A. 1993. *Ap. J.* 411:439
Simons DA, Becklin EE. 1992. *Ap. J.* 390:431.
Skrutskie MF, Shure M, Beckwith S. 1985. *Ap. J.* 299:303
Smecker TA, Wyse RFG. 1991. *Ap. J.* 372:448
Smoot GF, Bennett CL, Kogut A, Wright EL, Aymon J, et al. 1992. *Ap. J. Lett.* 396:L1
Speanhauer A, Jones BF, Whitford AE. 1992. *Astron. J.* 103:297
Spitzer L. 1958. *Ap. J.* 127:17
Steele IA, Jameson RF, Hambly NC. 1993. *MNRAS* 263:467
Steidel CC, Sargent WLW. 1988. *Ap. J. Lett.*

333:L5
Stevenson DJ. 1986. In *Astrophysics of Brown Dwarfs,* ed. MC Kafatos, RS Harrington, SP Maran, p. 66. Cambridge:Cambridge Univ. Press
Stevenson DJ. 1991. *Annu. Rev. Astron. Astrophys.* 29:163
Stromgren B. 1987. In *The Galaxy,* ed. G Gilmore, R Carswell, p. 229. Dordrecht:Reidel
Subramanian K, Chitre SM. 1987. *Ap. J.* 313:13
Suntzeff NB. 1992. In *The Stellar Populations of Galaxies,* ed. B Barbuy, A Renzini, p. 15. Dordrecht:Kluwer
Surdej J, Claeskens JF, Crampton D, Filippenko AV, Hutsemekers D, et al. 1993. *Astron. J.* 105:2064
Tamanaha CM, Silk J, Wood MA, Winget DE. 1990. *Ap. J.* 358:164
Taylor AN, Rowan-Robinson M. 1992. *Nature* 359:396
Terlevich RJ. 1985. In *Star Forming Dwarf Galaxies,* ed. D Kunth, TX Thuan, J Tran Thanh Van, p. 395. Paris:Editions Frontieres
Teuben PJ. 1991. In *Warped Disks and Inclined Rings Around Galaxies,* ed. S Casertano, PD Sackett, F Briggs, p. 40. Provo:Brigham Young Univ. Press
Thomas P, Fabian AC. 1990. *MNRAS* 246:156
Thorstensen JR, Partridge RB. 1975. *Ap. J.* 200:527
Tinney CG. 1993. *Ap. J.* 414:379
Tinney CG, Mould JR, Reid IN. 1992. *Ap. J.* 396:173
Tinney CG, Reid IN, Mould JR. 1993. *Ap. J.* 414:254
Tohline JE. 1980. *Ap. J.* 239:417
Trimble V. 1987. *Annu. Rev. Astron. Astrophys.* 25:425
Truran JW. 1984. *Annu. Rev. Nucl. Part. Phys.* 34:53
Truran JW, Cameron AGW. 1971. *Astrophys. Space Sci.* 14:179
Turner EL. 1980. *Ap. J. Lett.* 242:L135
Turner EL, Wardle MJ, Schneider DP. 1990. *Astron. J.* 100:146
Turner MS. 1991. *Phys. Scr.* T36:167
Udalski A, Szymanski M, Kaluzny J, Kubiak M, Krzeminski W, et al. 1993. *Acta Astron.* 43:289
Umemura M, Loeb A, Turner EL. 1993. *Ap. J.* 419:459
Valentijn EA. 1990. *Nature* 346:153
Van den Bergh S. 1969. *Nature* 224:891
Van der Kruit PC. 1987. In *Dark Matter in the Universe,* ed. GR Knapp, J Kormendy, p. 415. Dordrecht:Reidel
Vietri M, Ostriker JP. 1983. *Ap. J.* 267:488
Walker T, Steigman G Schramm DN, Olive KA, Kang HS. 1991. *Ap. J.* 376:51
Wambsganss J, Paczynski B. 1992. *Ap. J. Lett.* 397:L1
Wambsganss J, Paczynski B, Schneider P. 1990. *Ap. J. Lett.* 358:L33
Wandel A. 1985. *Ap. J.* 294:385
Wasserman I, Weinberg MD. 1987. *Ap. J.* 312:390
Wasserman I, Salpeter EE. 1993. Preprint
Webster RL, Fitchett M. 1986. *Nature* 324:617
Webster RL, Hewett PC, Harding ME, Wegner GA. 1988. *Nature* 336:358
Webster RL, Ferguson AMN, Corrigan RT, Irwin MJ. 1991. *Astron. J.* 102:1939
Wheeler JC, Sneden. C, Truran J. 1989. *Annu. Rev. Astron. Astrophys.* 27:279
White DA, Fabian AC, Johnstone RM, Mushotzky RF, Arnaud KA. 1991. *MNRAS* 252:72
White SDM. 1976. *MNRAS* 174:19
White SDM, Frenk CS. 1991. *Ap. J.* 379:52
White SDM, Navarro JF, Evrard AE, Frenk CS. 1993. *Nature* 366:429
White SDM, Rees MJ. 1978. *MNRAS* 183:341
Whitmore BC, McElroy DB, Schweizer F. 1987. *Ap. J.* 314:439
Wielen R. 1985. In *Dynamics of Star Clusters,* ed. J Goodwin, P Hut, p. 449. Dordrecht:Reidel
Wollmann ER. 1992. *Ap. J.* 392:80
Woosley SE, Weaver TA. 1982. In *Supernovae: A Survey of Current Research,* ed. MJ Rees, RJ Stoneham, p. 79. Dordrecht:Reidel
Wright EL. 1982. *Ap. J.* 255:401
Wright EL, Malkan MA. 1987. *Bull. Am. Astron. Soc.* 19:699
Wright EL, Mather JC, Fixen DJ, Kogut A, Schafer RA. 1994. *Ap. J.* 420:450
Yang J, Turner MS, Steigman G, Schramm DN, Olive K. 1984. *Ap. J.* 281:493
Yoshii Y, Saio H. 1986. *Ap. J.* 301:587
Zaritsky D, Smith R, Frenk CS, White SDM. 1993. *Ap. J.* 405:464
Zeldovich YaB. 1970. *Astron. Astrophys.* 5:84